Metabolic Engineering 52 (2019) 153–167

Contents lists available at ScienceDirect

Metabolic Engineering

journal homepage: www.elsevier.com/locate/meteng

aMSGE: advanced multiplex site-specific genome engineering with orthogonal modular recombinases in actinomycetes

Lei Li[a], Keke Wei[b,c], Xiaocao Liu[a,d], Yuanjie Wu[c], Guosong Zheng[a], Shaoxin Chen[c], Weihong Jiang[a,e,*], Yinhua Lu[f,**]

[a] Key Laboratory of Synthetic Biology, CAS Center for Excellence in Molecular Plant Sciences, Institute of Plant Physiology and Ecology, Chinese Academy of Sciences, Shanghai 200032, China
[b] School of Pharmacy, Fudan University, Shanghai 201203, China
[c] Department of Biochemistry, Shanghai Institute of Pharmaceutical Industry, Shanghai 201210, China
[d] School of Life Science, Henan University, Kaifeng 475004, China
[e] Jiangsu National Synergetic Innovation Center for Advanced Materials, SICAM, Nanjing 210009, China
[f] College of Life Sciences, Shanghai Normal University, Shanghai 200232, China

ARTICLE INFO

Keywords:
Site-specific recombination
Multi-copy integration
Actinomycetes
Natural product
Biosynthetic gene cluster (BGC)

ABSTRACT

Chromosomal integration of genes and pathways is of particular importance for large-scale and long-term fermentation in industrial biotechnology. However, stable, multi-copy integration of long DNA segments (e.g., large gene clusters) remains challenging. Here, we describe a plug-and-play toolkit that allows for high-efficiency, single-step, multi-locus integration of natural product (NP) biosynthetic gene clusters (BGCs) in actinomycetes, based on the innovative concept of "multiple integrases-multiple *attB* sites". This toolkit consists of 27 synthetic modular plasmids, which contain single- or multi-integration modules (from two to four) derived from five orthogonal site-specific recombination (SSR) systems. The multi-integration modules can be readily ligated into plasmids containing large BGCs by Gibson assembly, which can be simultaneously inserted into multiple native *attB* sites in a single step. We demonstrated the applicability of this toolkit by performing stabilized amplification of acetyl-CoA carboxylase genes to facilitate actinorhodin biosynthesis in *Streptomyces coelicolor*. Furthermore, using this toolkit, we achieved a 185.6% increase in 5-oxomilbemycin titers (from 2.23 to 6.37 g/L) in *Streptomyces hygroscopicus* via the multi-locus integration of the entire 5-oxomilbemycin BGC (72 kb) (up to four copies). Compared with previously reported methods, the advanced multiplex site-specific genome engineering (aMSGE) method does not require the introduction of any modifications into host genomes before the amplification of target genes or BGCs, which will drastically simplify and accelerate efforts to improve NP production. Considering that SSR systems are widely distributed in a variety of industrial microbes, this novel technique also promises to be a valuable tool for the enhanced biosynthesis of other high-value bioproducts.

1. Introduction

Industrial biotechnology is reliant on the approaches of native gene/pathway engineering or heterologous gene/pathway introduction for the cost-efficient biosynthesis of molecules of interest (Lee and Kim, 2015; Luo et al., 2015; Nielsen and Keasling, 2016). Chromosomal integration of genes/pathways is an imperative step to develop stable microbial cell factories that meet economic requirements for large-scale industrial production. However, chromosome-based expression is generally weak due to low copy numbers relative to plasmid-based systems. To achieve a high expression level, genes or metabolic pathways can be introduced into host genomes in multiple copies under the control of strong promoters. In general, two distinct principles, namely, site-specific recombination (SSR) and homologous recombination (HR), have been employed to achieve genomic integration of genes/pathways in a wide variety of microbial systems (Court et al., 2002; Fogg et al., 2014; Grindley et al., 2006). As a representative case, single-step, markerless and multi-locus integration of up to 18 copies of the xylose utilization and butanediol production pathway (24 kb) was successfully achieved by CRISPR-Cas9-assisted homology-directed repair (HDR) in

* Corresponding author at: Key Laboratory of Synthetic Biology, CAS Center for Excellence in Molecular Plant Sciences, Institute of Plant Physiology and Ecology, Chinese Academy of Sciences, Shanghai 200032, China.
** Corresponding author.
E-mail addresses: whjiang@sibs.ac.cn (W. Jiang), yhlu@shnu.edu.cn (Y. Lu).

https://doi.org/10.1016/j.ymben.2018.12.001
Received 17 October 2018; Received in revised form 27 November 2018; Accepted 4 December 2018
Available online 05 December 2018

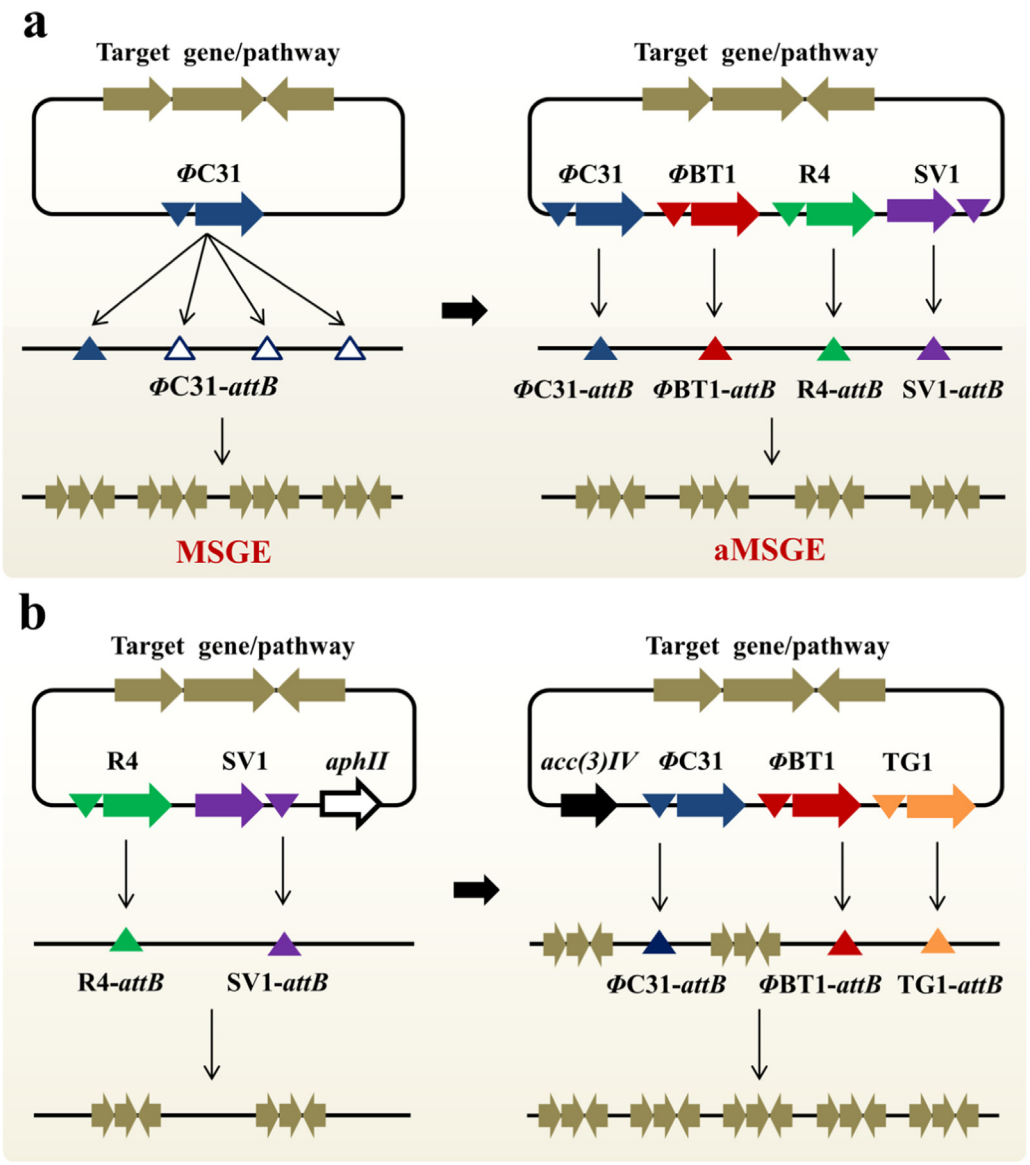

Fig. 1. Design principle of aMSGE. (a) In the MSGE method we previously developed based on the concept of 'one integrase-multiple *attB* sites', artificial *attB* sites (hollow triangle) must be iteratively introduced beforehand for targeted amplification of genes or pathways. However, in the aMSGE method based on the innovative concept of 'multiple integrases-multiple *attB* sites', these discrete *attB* sites are naturally occurring. (b) Two-round iterative multi-copy integration (up to five copies) of genes/pathways by means of interlaced resistance markers (*aphII* and *acc(3)IV*).

Saccharomyces cerevisiae (Shi et al., 2016). However, HDR-mediated integration is generally insufficient for manipulating large metabolic pathways, such as natural product (NP) biosynthetic gene clusters (BGCs, 10–100 kb) in filamentous fungi and actinomycetes (Li et al., 2017a; Smanski et al., 2016).

As an attractive alternative, SSR-mediated integration has been widely exploited for stable amplification of large metabolic pathways in actinomycetes and other important industrial microbes (Baltz, 2012; Merrick et al., 2018; Stark, 2017). In most cases, only one copy of a target pathway is introduced by using a single bacteriophage integration system, and thus the range of yield improvement is often limited. Recently, orthogonal integration systems have been iteratively employed to duplicate or triplicate natural product BGCs in actinomycetes (Haginaka et al., 2014). However, this approach involves repeated rounds of plasmid construction and conjugal transfer and is limited by the number of selection markers. To overcome these bottlenecks, we previously developed the MSGE method based on the concept of 'one integrase-multiple *attB* sites', which allows for efficient amplification of target BGCs in actinomycetes (Fig. 1a) (Li et al., 2017b). This method is highly suitable for the development of heterologous superhosts for the discovery of novel drug leads (Niu, 2018; Zhang et al., 2016), but it still has some limitations, which has hampered its broad application. On one hand, repeated insertion of artificial *attB* sites is laborious and time-consuming, even using CRISPR-based genome editing tools (Choi and Lee, 2016; Donohoue et al., 2018). On the other hand, it is very difficult to introduce artificial *attB* sites into the genomes of genetically intractable industrial actinomycetes (Shapiro et al., 2018; Weber et al., 2015). Therefore, it is crucial to establish a novel and general approach for stable, efficient and single-step amplification of large metabolic pathways in actinomycetes.

As the main production strains for naturally derived drugs, actinomycetes have historically made significant contributions to human health and crop protection and will continue to be important sources for the discovery of novel bioactive natural products (Barka et al., 2016; Butler et al., 2014; Nepal and Wang, 2018). In general, actinomycete genomes contain no or only one active chromosomal *attB* site for each bacteriophage integration system (Baltz, 2012). However, there is a large number of SSR systems with broad host ranges in actinomycetes,

Table 1
The 27 modular plasmids in the plug-and-play toolkit for single-step or iterative multi-copy integration of target genes or BGCs in actinomycetes.

Name	Genbank accession numbers	Integrases	Marker	Descriptions
pSET152	AJ414670	ΦC31	*acc(3)IV*	For systematic verification of accessible site-specific integration systems in a specific actinomycete strain
pRT801	MH192349	ΦBT1	*acc(3)IV*	
pLR4	MK190411	R4	*acc(3)IV*	
pLSV1	MK190412	SV1	*acc(3)IV*	
pLTG1	MK190413	TG1	*acc(3)IV*	
pLB1	MK159854	ΦBT1	*acc(3)IV*	Single-integration modular plasmids with universal assembly overlaps and the super-strong promoter *kasOp**
pLC1	MK159855	ΦC31	*acc(3)IV*	
pLB2	MK159853	ΦBT1	*aphII*	
pLS2	MK159852	SV1	*aphII*	
pLCB1	MK176918	ΦC31, ΦBT1	*acc(3)IV*	Dual-integration modular plasmids with universal assembly overlaps and the super-strong promoter *kasOp**
pLCT1	MK176919	ΦC31, TG1	*acc(3)IV*	
pLBT1	MK176920	ΦBT1, TG1	*acc(3)IV*	
pLBR2	MK176921	ΦBT1, R4	*aphII*	
pLBS2	MK176922	ΦBT1, SV1	*aphII*	
pLSR2	MK176923	SV1, R4	*aphII*	
pLCBR1	MK176924	ΦC31, ΦBT1, R4	*acc(3)IV*	Triple-integration modular plasmids with universal assembly overlaps and the super-strong promoter *kasOp**
pLCBS1	MK176925	ΦC31, ΦBT1, SV1	*acc(3)IV*	
pLCBT1	MK176926	ΦC31, ΦBT1, TG1	*acc(3)IV*	
pLSRB2	MK176927	SV1, R4, ΦBT1	*aphII*	
pLSRC2	MK176928	SV1, R4, ΦC31	*aphII*	
pLSRT2	MK176929	SV1, R4, TG1	*aphII*	
pLCBRS1	MK176930	ΦC31, ΦBT1, R4, SV1	*acc(3)IV*	Quadruple-integration modular plasmids with universal assembly overlaps and the super-strong promoter *kasOp**
pLCBRT1	MK176931	ΦC31, ΦBT1, R4, TG1	*acc(3)IV*	
pLCBST1	MK176932	ΦC31, ΦBT1, SV1, TG1	*acc(3)IV*	
pLSRBC2	MK176933	SV1, R4, ΦBT1, ΦC31	*aphII*	
pLSRBT2	MK176934	SV1, R4, ΦBT1, TG1	*aphII*	
pLSRCT2	MK176935	SV1, R4, ΦC31, TG1	*aphII*	

such as the ΦC31, ΦBT1 and TG1 integration systems (Baltz, 2012). In the past decades, integration systems have been widely employed to facilitate genetic engineering (Baltz, 2012; Merrick et al., 2018), DNA assembly (Colloms et al., 2014; Zhang et al., 2011) as well as the construction of logic gates (Bonnet et al., 2013; Roquet et al., 2016) and data storage devices (Siuti et al., 2013; Yang et al., 2014). Using a series of orthogonal modular integration systems and native *attB* sites, here we developed a plug-and-play toolkit for rapid and stable amplification of genes or large BGCs in actinomycetes (Fig. 1 and Table 1). We expect that this multi-copy integration toolkit will facilitate our efforts to improve the biosynthesis of important nature-derived drugs in actinomycetes. Additionally, considering that SSR systems are distributed in a wide variety of industrial microorganisms, including *Escherichia coli*, *Bacillus*, *Clostridium*, and *Lactococcus* (Fogg et al., 2014; Smith, 2015; St-Pierre et al., 2013; Yang et al., 2014), we believe that this novel multi-copy integration methodology will be widely applicable to efficiently improve the biosynthesis of other value-added biomolecules.

2. Results

2.1. Design principle of aMSGE

Here, we aim to develop an advanced MSGE method (aMSGE) based on the innovative concept that multiple orthogonal integration systems can mediate the simultaneous insertion of genes/pathways into corresponding native *attB* sites in actinomycete genomes in a single step ("multiple integrase-multiple *attB* sites") (Fig. 1a). In this novel method, a plug-and-play toolkit containing 27 modular plasmids, which contain single- or multi-integration modules (from two to four) derived from five orthogonal SSR systems, was established (Table 1). According to the size of the integrated DNA constructs, two different strategies were adopted to construct the plasmids containing target genes/pathways and multi-integration modules. When genes/pathways are less than ~15 kb, they can be directly ligated into the modular plasmids containing multi-integration modules. In contrast, when target genes or pathways are larger (e.g., 15–100 kb), multi-integration modules can be added into the plasmids containing large metabolic pathways by Gibson assembly (Gibson et al., 2009). Furthermore, an iterative integration strategy was also designed to easily achieve the insertion of large metabolic pathways with up to five copies in two steps (Fig. 1b). The procedure only takes ~2 days for plasmid editing and ~15 days for the construction of engineered strains (e.g., strain growth period is ~5 days), which drastically simplifies and accelerates efforts to achieve stable amplification of target genes/pathways for enhanced production of high-value biomolecules.

2.2. Design, build and test of the plug-and-play toolkit for multi-locus integration of target genes/pathways

Until now, at least nine SSR systems have been identified in actinomycetes, including the ΦC31 (Lomovskaya et al., 1972), ΦBT1 (Gregory et al., 2003), R4 (Chater and Carter, 1979), SV1 (Fayed et al., 2014), TG1 (Morita et al., 2009), VWB (Van Mellaert et al., 1998), ΦJoe (Fogg et al., 2017), ΦK38-1 (Yang et al., 2014), and CBG73463 (Yang et al., 2014) integration systems. The detailed *attB* and *attP* sequences of these systems are listed in Fig. S1. To construct the plug-and-play, multi-copy integration toolkit, five compatible integration systems (ΦC31, ΦBT1, R4, SV1 and TG1 integrases & *attP* sites) were selected due to their broad host range based on the reported literature and bioinformatics analysis (Figs. 2 and S2) (Baltz, 2012). First, five plasmids consisting of a single integration system and an apramycin resistance marker, including pSET152 (ΦC31), pRT801 (ΦBT1), pLR4 (R4), pLSV1 (SV1) and pLTG1 (TG1), were selected and constructed to test whether these recombination systems could efficiently mediate genomic integration in different actinomycetes (Table 1). Three *Streptomyces* strains, including the model strain *Streptomyces coelicolor* M145 and two important industrial strains, pristinamycin-producing *Streptomyces pristinaespiralis* HCCB10218 and 5-oxomilbemycin-producing *Streptomyces hygroscopicus* SIPI-KF, were selected. Then, the integration efficiencies of these five plasmids were systematically determined in the three tested *Streptomyces* strains. Two *Escherichia coli* strains, the methylation-deficient ET12567/pUZ8002 and methylation-proficient S17-1, were selected as donors. As shown in Fig. S3, in *S. coelicolor*, the R4 recombination system (cloned in pLR4) showed the lowest integration

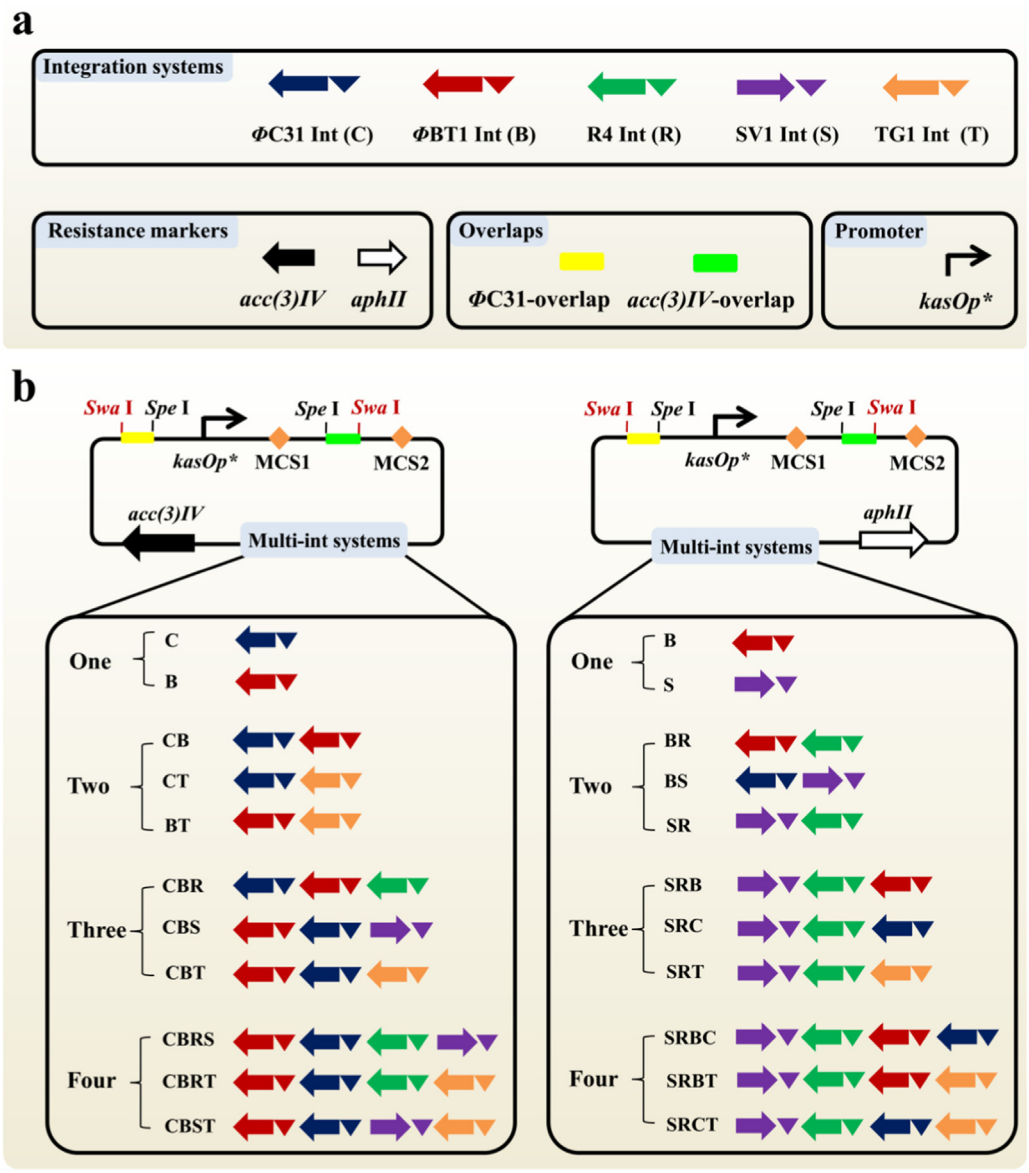

Fig. 2. Design of the plug-and-play toolkit for multi-copy integration of genes or pathways. (a) The standard biological parts in this toolkit, including five orthogonal site-specific integration systems (each contains an integrase gene and a corresponding *attP* site), two drug resistance markers and two universal assembly overlaps as well as one super-strong promoter *kasOp**. (b) Design of a plasmid library containing different combinations of multi-integration systems. Two different sets of modular plasmids, including one, two, three or four orthogonal integration systems, were constructed based on two compatible resistance markers, *aphII* and *acc(3)IV*. Notably, the number "1" in the plasmids pLC1 and pLB1 represents the *acc(3)IV* resistance marker, while the number "2" in the plasmids pLB2 and pLS2 represents the *aphII* resistance marker. MCS1 (*Bam*HI and *Pac*I) and MCS2 (*Pme*I, *Nsi*I, *Not*I and *Mfe*I) were employed to clone small genes/pathways and construct modular plasmids containing different orthogonal integration systems, respectively. Two restriction enzyme sites (*Spe*I and *Swa*I) were inserted into the respective sides of the assembly overlaps to facilitate the addition of multiple integration systems into plasmids containing large metabolic pathways.

efficiency among the five site-specific recombination systems, and ET12567/pUZ8002 was the better donor strain relative to S17-1. In *S. pristinaespiralis* or *S. hygroscopicus*, all five tested plasmids showed approximately equivalent integration efficiencies. Collectively, these results indicated that the five integration systems we selected could indeed work well in the above three *Streptomyces* strains and were suitable for the construction of the plug-and-play toolkit.

In addition to five orthogonal integration systems, this toolkit also contains two interlaced drug resistance markers (*acc(3)IV* and *aphII*), one super-strong engineered promoter *kasOp** and two universal assembly overlaps (*Φ*C31-overlap and *acc(3)IV*-overlap) (Fig. 2a). Two drug resistance markers were introduced for the following iterative integration of target genes or BGCs, allowing for multi-copy integration in two rounds. The promoter *kasOp** was previously demonstrated to exhibit stronger activity than the commonly used *ermEp** in multiple *Streptomyces* strains (W.S. Wang et al., 2013). Therefore, it can be directly employed for the overexpression of target genes in plasmids with multi-integration modules. The design of two universal 38-bp overlaps could facilitate the subsequent editing of plasmids with large BGCs by Gibson assembly. Generally, target BGCs are captured or assembled into widely used cloning vectors, such as pTARa (Kim et al., 2010), pSBAC (Liu et al., 2009) and pHL921 (Xu et al., 2016), all of which contain the same integration-resistance (IR) cassette, *Φ*C31-*acc(3)IV*. To realize iterative chromosomal integration of target BGCs, the *Φ*C31-*acc(3)IV* cassette could be replaced by new integration modules (containing the *aphII* resistance marker and different numbers of integration systems) using the in vitro DNA editing method (the CGE method) we developed previously (Li et al., 2017b). The *Φ*C31-*acc(3)IV* IR cassette was removed by the endonuclease Cas9 with the help of two sgRNAs (*Φ*C31-sgRNA and *acc(3)IV*-sgRNA) targeting the *Φ*C31 integrase gene and the *acc(3)IV* gene, respectively (Fig. 3a). The 38-bp terminal sequences (hooks) of the linearized plasmids were designed as PCR primers and then introduced into the two ends of the multi-integration cassettes beforehand. Additionally, two interlaced restriction enzyme sites (*Spe*I and *Swa*I) were designed and introduced into the respective sides of the designed overhangs.

After carefully defining all starting functional modules, we began to design, build and test the plug-and-play toolkit (Table 1). To achieve iterative integration of target genes or BGCs, we constructed two series of modular plasmids with the *aac(3)IV* and *aphII* resistance markers, respectively. The experimental setup and procedure were as follows. First, four single-integration plasmids, including two with the *aac(3)IV* resistance marker (pLC1 and pLB1) and two with the *aphII* resistance marker (pLB2 and pLS2), were constructed from the plasmids pSET152

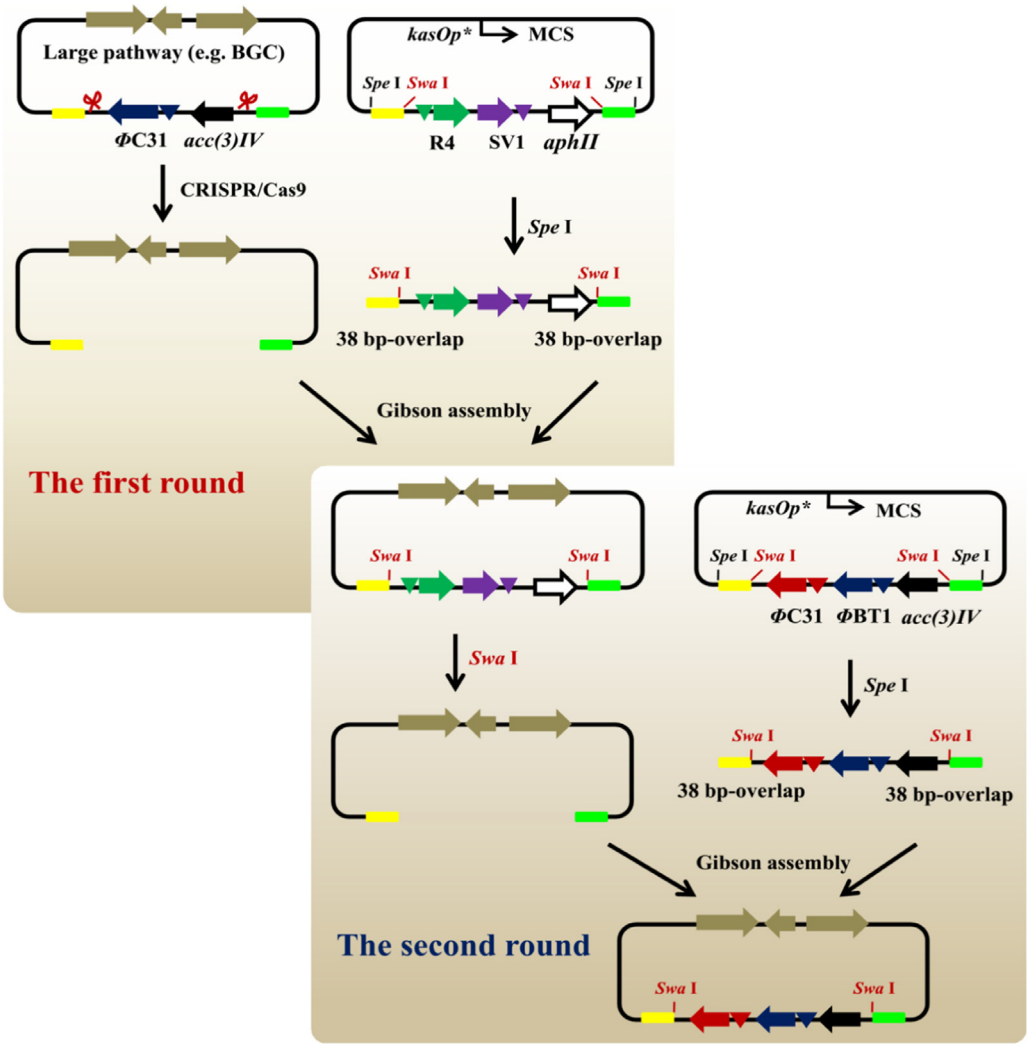

Fig. 3. Iterative introduction of multiple integration systems into plasmids containing large metabolic pathways. In the first round, the in vitro CRISPR-Cas9 system is employed to remove integration-resistance (IR) cassettes in the starting editing plasmids. In the second round, the restriction enzyme *Swa*I is used to remove the original IR cassettes. Notably, *Swa*I may be present in some specific biosynthetic pathways, and thus other restriction enzyme sites should be introduced to replace the pre-design site. Finally, the Gibson assembly method is employed to add multiple integration systems into plasmids containing large biosynthetic pathways. MCS represents multiple cloning sites.

Table 2
Multi-copy integration efficiencies of a panel of modular plasmids containing two (a), three (b) and four (c) orthogonal site-specific recombination systems in the model strain *S. coelicolor* M145 and the industrial strain *S. pristinaespiralis* HCCB10218. ND: not detected.

(a)	pLBT1	pLCB1	pLCT1	pLBR2	pLBS2	pLSR2
M145	100% (10/10 + 10/10)	95% (9/10 + 10/10)	90% (8/10 + 10/10)	90% (9/10 + 9/10)	75% (9/10 + 6/10)	90% (9/10 + 9/10)
HCCB10218	40% (4/10 + 4/10)	80% (9/10 + 7/10)	60% (8/10 + 4/10)	35% (4/10 + 3/10)	45% (6/10 + 3/10)	100% (10/10 + 10/10)

(b)	pLCBR1	pLCBS1	pLCBT1	pLSRB2	pLSRC2	pLSRT2
M145	100% (10/10 + 10/10)	100% (10/10 + 10/10)	100% (10/10 + 10/10)	75% (8/10 + 7/10)	80% (8/10 + 8/10)	65% (9/10 + 4/10)
HCCB10218	25% (3/10 + 2/10)	0% (0/10 + 0/10)	0% (0/10 + 0/10)	0% (0/10 + 0/10)	ND	ND

(c)	pLCBRS1	pLCBRT1	pLCBST1	pLSRBC2	pLSRBT2	pLSRCT2
M145	90% (9/10 + 9/10)	30% (3/10 + 3/10)	30% (3/10 + 3/10)	0% (0/10 + 0/10)	0% (0/10 + 0/10)	0% (0/10 + 0/10)
HCCB10218	ND	ND	ND	ND	ND	ND

and pRT802, respectively. The four plasmids contained a single-integration system (*Φ*C31, *Φ*BT1 or SV1 integrase/*attP*), two universal assembly overhangs, the promoter *kasOp** and two series of multiple cloning sites (MCS1 and MCS2). Notably, the number "1" in the plasmids pLC1 and pLB1 represents the *acc(3)IV* resistance marker, while the number "2" in the plasmids pLB2 and pLS2 represents the *aphII* resistance marker. Based on pLC1 and pLB1, three plasmids with the *acc(3)IV* resistance marker and different combinations of two integration modules, namely, pLCB1, pLCT1 and pLBT1, were constructed via the addition of the *Φ*BT1 and TG1 integration systems. Similarly, three plasmids with the *aphII* resistance marker and three different combinations of two integration modules, namely, pLBR2, pLBS2 and pLSR2, were constructed by introducing the R4 and SV1 integration systems into the plasmids pLB2 and pLS2. Then, we tested the insertion efficiencies of these six plasmids with different combinations of two different integration systems in *S. coelicolor* and *S. pristinaespiralis*. All six plasmids were efficiently integrated into the two corresponding *attB* sites with at least 75% efficiency in *S. coelicolor* (Fig. S4 and Table 2a). However, insertion efficiencies were very different when the six plasmids were introduced into *S. pristinaespiralis*. Among the *acc(3)IV*- and

aphII-marked plasmids, pLCB1 (containing the ΦC31 and ΦBT1 integration systems) and pLSR2 (containing the SV1 and R4 integration systems) showed the highest two-copy integration efficiencies (Fig. S5 and Table 2a). Therefore, the plasmids pLCB1 and pLSR2 were chosen to further construct plasmids with three integration modules.

Three plasmids with the *acc(3)IV* resistance marker and different combinations of three integration modules, pLCBR1, pLCBS1 and pLCBT1, were constructed by introducing the R4, SV1 and TG1 integration systems into the plasmid pLCB1. Similarly, the ΦC31, ΦBT1 and TG1 integration systems were added into the plasmid pLSR2, thus generating the plasmids pLSRB2, pLSRC2 and pLSRT2 with the *aphII* resistance marker and different combinations of three integration modules. Again, we systematically tested the insertion efficiencies of these six plasmids with three integration modules in *S. coelicolor* and *S. pristinaespiralis*. In *S. coelicolor*, the three *acc(3)IV*-marked plasmids showed 100% efficiency for three-locus simultaneous integration, and the three *aphII*-marked plasmids also showed 65–80% efficiencies for three-locus simultaneous integration (Fig. S6 and Table 2b). Phenotypic analysis showed that three-copy chromosomal integration of either pLSRC2 or pLSRT2 led to poor growth on MS agar plates (Fig. S7a), indicating combinatorial overexpression of either the SV1/R4/ΦC31 or SV1/R4/TG1 integration systems was toxic to bacterial growth. However, in *S. pristinaespiralis*, simultaneous insertion of three orthogonal integration systems into the corresponding native *attB* sites was very difficult. Only the plasmid pLCBS1 could be integrated into the chromosome with three copies at an efficiency of 20% (Fig. S8 and Table 2b).

Finally, we constructed two series of plasmids with four integration modules, including three with the *aac(3)IV* resistance marker (pLCBRS1, pLCBRT1, and pLCBST1) and three with the *aphII* resistance marker (pLSRBC2, pLSRBT2 and pLSRCT2), using the same strategy. In *S. coelicolor*, the plasmid pLCBRS1 showed the highest four-copy simultaneous integration efficiency (90%) among all tested six plasmids. The three *aphII*-marked plasmids, pLSRBC2, pLSRBT2 and pLSRCT2, could not be inserted into the chromosome with four copies (Fig. S9 and Table 2c). Phenotypic analysis showed that four-copy chromosomal integration of pLCBRT1 and pLCBST1 led to poor bacterial growth on MS agar plates (Fig. S7b). Collectively, these results indicate that the aMSGE method enabled simultaneous four-copy chromosomal integration of DNA constructs in *S. coelicolor*, especially using the plasmid pLCBRS1. However, in *S. pristinaespiralis*, this novel method only allowed for a maximum of three-copy chromosomal integration of DNA constructs.

Afterwards, we attempted to achieve four-copy DNA integration by two-round iterative integration. It was observed that the modular plasmids containing two integration systems (pLBT1, pLCB1 and pLCT1) could be efficiently inserted into the two corresponding *attB* sites with almost 100% efficiency in *S. coelicolor* M145 containing two other orthogonal integration systems (pLBR2, pLBS2 and pLSR2) (Fig. S10 and Table 3). Notably, introduction of the plasmid pLCT1 into M145/pLSR2 led to poor bacterial growth on MS agar plates (Fig. S7c), further confirming that combinatorial overexpression of four integration systems (ΦC31/TG1/SV1/R4) was toxic to bacterial growth. On the other hand, the plasmid pLSR2 could also be integrated into two corresponding *attB* sites in *S. pristinaespiralis* HCCB10218 containing two other orthogonal integration systems (pLBT1, pLCB1 and pLCT1) with high efficiency. However, when the plasmid pLBR2 was introduced into 10218/pLCT1, two-copy integration efficiency was only 20% (3/10 + 1/10) (Fig. S11 and Table 3). Similarly, we found that introduction of the plasmid pLBS2 introduced into 10218/pLCT1 resulted in poor bacterial growth on RP agar plates (Fig. S7d). Collectively, the multi-copy integration toolkit could be employed for rapid and stable amplification of target genes/pathways in a single step or in two steps in actinomycetes.

Herein, we provide a simple guideline to quickly use this plug-and-play toolkit for stable amplification of genes/pathways. First, the five plasmids (pSET152, pRT801, pLSV1, pLR4 and pLTG1) should be directly used to identify accessible SSR systems in a specific actinomycete strain. Second, different modular plasmids are carefully chosen to mediate multi-copy integration of genes/pathways in a single-step or two-round iterative manner. These universal plasmids in the toolkit are comprehensively shown in Fig. 2b and Table 1.

2.3. Iterative replacement of multi-integration systems in cloning vectors containing large metabolic pathways

As mentioned above, large metabolic pathways, such as natural product BGCs, are usually cloned or assembled into single integration system (e.g., ΦC31)-based cloning vectors. To rapidly achieve multi-copy integration of target pathways in a single step, multi-integration systems could be added into cloning vectors by using the CGE method beforehand (Li et al., 2017b). Briefly, the original ΦC31-*acc(3)IV* IR cassette in cloning vectors was removed by Cas9 with ΦC31-sgRNA and *acc(3)IV*-sgRNA (Fig. 3). Then, new IR cassettes, e.g., the R4-SV1-*aphII* cassette, were obtained by digesting the modular plasmids with *Spe*I, and then ligated into the linearized vector by Gibson assembly. It is worth noting that some cloning vectors, such as pCAP01 (Yamanaka et al., 2014) and pCC1BAC (Gibson et al., 2009), do not contain the ΦC31-*acc(3)IV* cassette. Therefore, new sgRNAs should be designed to linearize cloning vectors and remove original IR cassettes, if they exist. Additionally, in this case, the universal overlaps, ΦC31-overlap and *acc(3)IV*-overlap, can no longer be used, and modular IR cassettes with new assembly overlaps should be obtained by PCR amplification using high-fidelity DNA polymerases.

To realize multi-round integration of large biosynthetic pathways, we also designed an iterative strategy for the repeat addition of modular IR cassettes into cloning vectors. As shown in Fig. 3, a *Swa*I restriction enzyme site that does not exist in a cloning vector containing target pathways was introduced into two sides of the modular IR cassettes in advance. Therefore, the modular IR cassettes, such as the SV1-R4-*aphII* cassette, could be easily removed with *Swa*I during second-round plasmid editing. In this way, a variety of new sgRNAs do not need to be designed to remove different modular IR cassettes. Notably, *Swa*I may be present in some cloned BGCs, and thus other specific restriction enzyme sites should be introduced by PCR amplification using the plug-and-play plasmids as templates. Finally, orthogonal modular IR cassettes, such as ΦC31-ΦBT1-*acc(3)IV* IR cassette, were obtained by directly digesting the corresponding modular plasmids with *Spe*I, and ligated into the *Swa*I-digested vectors by Gibson assembly. Collectively, this design will efficiently achieve multi-round replacement of the modular IR cassettes in cloning vectors containing large metabolic pathways.

Table 3
Two-copy iterative integration efficiencies of a series of modular plasmids containing two orthogonal site-specific recombination systems in the model strain *S. coelicolor* M145 and the industrial strain *S. pristinaespiralis* HCCB10218. ND: not detected.

	pLBT1	pLCB1	pLCT1		pLBR2	pLBS2	pLSR2
M145/pLBR2	ND	ND	100% (10/10 + 10/10)	**10218/pLBT1**	ND	ND	90% (10/10 + 8/10)
M145/pLBS2	ND	ND	95% (10/10 + 9/10)	**10218/pLCB1**	ND	ND	95% (9/10 + 10/10)
M145/pLSR2	90% (9/10 + 9/10)	100% (10/10 + 10/10)	90% (9/10 + 9/10)	**10218/pLCT1**	20% (3/10 + 1/10)	ND	90% (9/10 + 9/10)

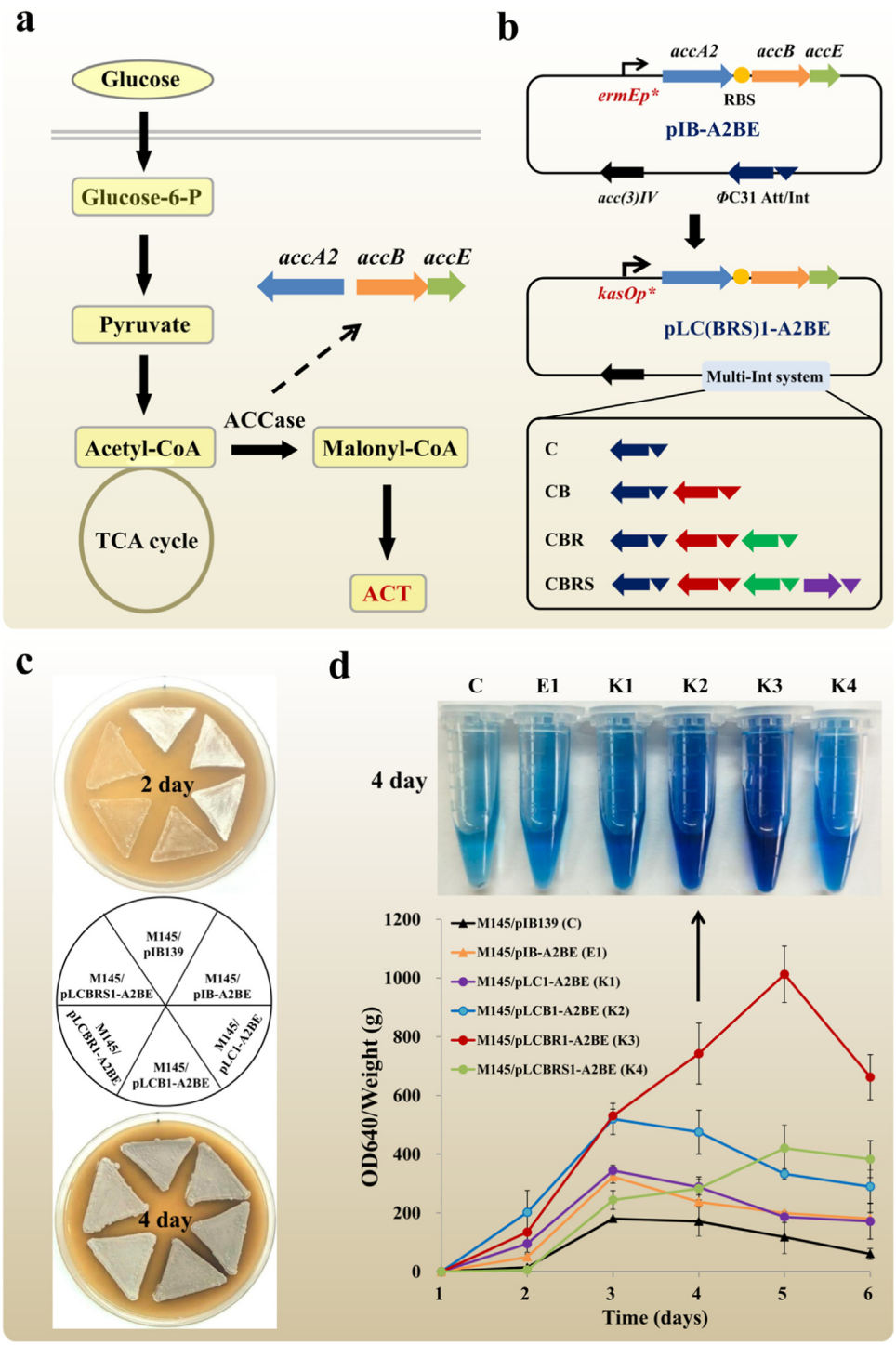

Fig. 4. Enhancement of actinorhodin (ACT) biosynthesis by aMSGE-mediated optimization of precursor supply in *S. coelicolor* M145. (a) Diagram of central carbon metabolism and intermediates for ACT production in *S. coelicolor*. Three genes (*accA2*, *accB* and *accE*) encoding acetyl-CoA carboxylase (ACCase) are responsible for transforming acetyl-CoA into malonyl-CoA (the main precursor of ACT biosynthesis). (b) Design of multi-copy genomic integration of the genes *accA2BE* under the control of the super-strong promoter *kasOp**. As a control, the strong promoter *ermEp** was employed to drive the expression of *accA2BE* in the plasmid pIB139 containing only the *Φ*C31 integration system. (c) Effects of *accA2BE* overexpression on bacterial growth on MS agar plates. The images were photographed from the front side at 2 and 4 days. (d) Effects of *accA2BE* overexpression on ACT biosynthesis on R2YE agar plates. The images (blue color in tubes) were photographed at 4 days. Samples were collected at five time points as indicated, and the experiments were performed in triplicate.

2.4. Optimization of precursor supply for actinorhodin biosynthesis by the aMSGE method

Generally, secondary metabolites from actinomycetes are classified into several families, including polyketides, non-ribosomal peptides and terpenes, etc. (Barka et al., 2016; Genilloud, 2017). A sufficient supply of precursors from primary metabolism is a key factor for the production of these secondary metabolites (Olano et al., 2008; Weber et al., 2015). One molecule of acetyl-CoA and seven molecules of malonyl-CoA are required to synthesize one molecule of the blue-colored actinorhodin ACT in *S. coelicolor* (Fig. 4a) (Ryu et al., 2006). Three genes (*accA2*, *accB* and *accE*), encoding acetyl-CoA carboxylase (ACCase) subunits, are responsible for converting acetyl-CoA to malonyl-CoA in *S. coelicolor* (Fig. 4a) (Ryu et al., 2006). Previously, overexpression of *accA2BE* under the control of the strong promoter *ermEp** using a single-copy integrative plasmid (pIB139) resulted in a significant increase in ACT production (Ryu et al., 2006). Here, as a case study, the aMSGE method was employed to strengthen ACCase expression to efficiently divert the carbon flux from acetyl-CoA to malonyl-CoA. A panel of plasmids containing different numbers of integration modules (from one to four) with high integration efficiencies from the plug-and-play toolkit, including pLC1, pLCB1, pLCBR1 and pLCBRS1, was used to express *accA2BE* under the control of the super-strong promoter *kasOp**, thus generating the plasmids pLC1-A2BE, pLCB1-A2BE,

pLCBR1-A2BE and pLCBRS1-A2BE, respectively. The plasmid pIB139, only containing the ΦC31 integration system, was also used to clone *accA2BE* under the control of *ermEp**, resulting in the plasmid pIB-A2BE. To assess the effects of the multi-copy integration of *accA2BE* on ACT biosynthesis, the above five plasmids and the empty plasmid pIB139 were individually introduced into *S. coelicolor* M145 by conjugal transfer. We found that these engineered plasmids could be integrated into all corresponding *attB* sites with almost 100% efficiency (Fig. S12). However, with the increased copy numbers of *accA2BE*, the growth of these engineered strains was gradually worse on MS agar plates (Fig. 4c), possibly due to ACCase overexpression (with four copies) diverting too much acetyl-CoA from the central metabolic pathway.

Subsequently, ACT production titers produced by these engineered strains were quantitatively determined (Kieser et al., 2000). The results showed that ACT production was significantly enhanced with the increase in copy numbers of *accA2BE* (Fig. 4d). M145/pLCBR1-A2BE (three extra copies of *accA2BE*) produced 2.1 and 4.6 times more ACT than M145/pIB-A2BE (one extra copy of *accA2BE*) and M145/pIB139 (empty control), respectively. However, M145/pLCBRS1-A2BE (four extra copies of *accA2BE*) exhibited delayed and lower ACT production relative to M145/pLCBR1-A2BE, which is mainly ascribed to the poor bacterial growth of the engineered strain with pLCBRS1-A2BE. In addition, although ACT production of M145/pLC1-A2BE (one extra copy of *accA2BE* under the control of *kasOp**) was higher than that of M145/pIB-A2BE (one extra copy of *accA2BE* under the control of *ermEp**) after 2 days of growth as expected [50.3 compared with 15 OD640/weight (g)], the highest ACT production of both engineered strains were the same after 3 days of growth. This might be due to the significantly decreased mRNA levels of these two strong promoters during later growth stages (60–96 h) of *S. coelicolor* (W.S. Wang et al., 2013). Nevertheless, these results clearly demonstrated that the aMSGE could achieve efficient multi-copy integration of ACCase genes for precursor supply optimization of ACT synthesis in a single step. Additionally, a series of multi-integration modular plasmids in the plug-and-play toolkit provide new and powerful alternatives to the conventional plasmid pIB139 for the strong overexpression of target genes in actinomycetes.

2.5. Enhancing 5-oxomilbemycin production by aMSGE-based BGC amplification in S. hygroscopicus SIPI-KF

In the present study, our main goal is to achieve stable, multi-copy integration of natural product BGCs for enhanced biosynthesis using the aMSGE method. Here, the 5-oxomilbemycin BGC (~72 kb) was chosen as an example. Produced by *S. hygroscopicus* SIPI-KF, 5-oxomilbemycin mainly consists of two chemically related molecules, 5-oxomilbemycin A3 and A4 (Takiguchi et al., 1980). Milbemycin oxime, the semi-synthetic derivative of 5-oxomilbemycin, has been approved to treat a broad range of agricultural pests and animal parasites (Bowman et al., 2014). In the BGC organization, 5-oxomilbemycin BGC is divided into two parts by a ~62-kb functionally unidentified DNA region, which includes the large part (from *milA2* to *milR*) and the small part (*milA1* and *milD*) (Fig. 5a) (Nonaka et al., 1999; Wang et al., 2010). Using Cas9-assisted TAR cloning technology (Lee et al., 2015), we successfully captured the two discrete parts of the 5-oxomilbemycin BGC into the cloning vector pCAP01a, thus generating the plasmids pCAP-*milA1* and pCAP-*milA2-R*, respectively (Fig. 5a). The cloned gene *milA1* and the gene cluster *milA2-R* were further verified by restriction analysis as shown in Fig. 5b.

To test the effects of these two parts on 5-oxomilbemycin production, pCAP-*milA1* and pCAP-*milA2-R* were individually introduced into SIPI-KF, generating the engineered strains KF101 and KF102. As a negative control, the empty plasmid pCAP01a was also introduced into SIPI-KF to generate the strain KF100. Notably, only a few exoconjugants (less than 10 colonies) grew out when the three plasmids described above were introduced (data not shown). Phenotypic analysis showed that the introduction of one extra copy of the gene *milA1* or the gene cluster *milA2-R* had no effect on bacterial growth on MB agar plates (Fig. S13). Fermentation analysis showed that individual introduction of pCAP-*milA1* and pCAP-*milA2-R* led to maximum increases in 5-oxomilbemycin biosynthesis of 69% (from 2271 to 3839 mg/L) and 79% (from 2271 to 4054 mg/L), respectively (Fig. 5c). Therefore, we attempted to simultaneously introduce *milA1* and *milA2-R* into SIPI-KF. Considering that pCAP-*milA1* and pCAP-*milA2-R* have the same ΦC31-*acc(3)IV* IR cassette, one of the two IR cassettes must be replaced by another IR cassette (e.g., the ΦBT1-*aphII* IR cassette) to facilitate simultaneous integration of both *milA1* and *milA2-R*. Thus, the gene *milA1* under the control of its own promoter from pCAP-*milA1* was first ligated into the plasmid pRT802, generating pRT802-*milA1*. Then, pRT802-*milA1* was integrated into KF102 (harbouring pCAP-*milA2-R*) to generate the engineered strain KF103, which contains both *milA1* and *milA2-R*. KF103 showed no obvious growth difference relative to KF100 on MB agar plates (Fig. S13). Fermentation analysis showed that the maximum 5-oxomilbemycin titer of KF103 was improved by 15% (from 4054 to 4654 mg/L) relative to that of KF102 (Fig. 5c).

To investigate the effects of the introduction of both *milA1* and *milA2-R* on 5-oxomilbemycin production at the transcriptional level, we compared the transcription of four 5-oxomilbemycin biosynthetic genes (*milA1*, *milA2*, *milA4* and *milR*) in KF101-KF103 with that of KF100. qRT-PCR analysis revealed that the transcription levels of *milA1* in KF101, the genes *milA2*, *milA4* and *milR* in KF102 and all four tested genes in KF103 were significantly enhanced upon chromosomal integration of the corresponding gene or gene cluster (Fig. 5d). The results clearly indicated that duplication of the 5-oxomilbemycin biosynthetic genes is a highly efficient strategy to enhance 5-oxomilbemycin production.

To obtain the entire 5-oxomilbemycin BGC for multi-copy chromosomal integration, we attempted to assemble *milA1* and *milA2-R* together in the vector pCAP01a using the TAR method. However, we failed despite several attempts. We reasoned that the pUC *ori* in pCAP01a could not stably carry such a large DNA fragment (Yamanaka et al., 2014), possibly due to excessive burden from high-copy large-size DNA replication. Therefore, we constructed a novel large gene cluster cloning vector, pCL01, based on the copy-control pCC1BAC plasmid. The copy number of pCC1BAC could be increased from one to 10–20 copies per cell by the addition of a copy-control inducer (Gibson et al., 2009). This feature will efficiently facilitate the capture of large gene clusters (> 100 kb) in the single-copy form and the enrichment of cloned gene clusters in the medium-copy form in *E. coli*. The vector pCL01 contains another two elements that permit plasmid screening and maintenance in yeast (the ARSH4/CEN6-TRP1 cassette) as well as the integration of target genes/pathways (the ΦC31-*acc(3)IV* IR cassette) in actinomycetes (Fig. S14a). Two restriction enzyme sites (*Eco*RI and *Pme*I) were also inserted into pCL01 to allow for the cloning of two homology arms (capture arms) corresponding to both ends of the target BGCs (Fig. S14a). Then, *milA1* and *milA2-R* were sequentially captured into the vector pCL01 by TAR cloning, thus generating the plasmid pCL01-milbe (Fig. 6a and S14b). The cloned entire 5-oxomilbemycin BGC was further verified by restriction analysis (Fig. 6b). However, intriguingly, we found that the plasmid pCL01-milbe could not be introduced into SIPI-KF (Fig. S14c), which might possibly be due to the large size of pCL01-milbe (87 kb) or the presence of the yeast element. To address this problem, a series of control plasmids were introduced into SIPI-KF, including pCL01, the empty plasmid BAC-F15 (F15 containing the ΦC31-*acc(3)IV* IR cassette), and the plasmid BAC-F1F15, with a large pristinamycin II BGC (81 kb) (Li et al., 2015). BAC-F15 and BAC-F1F15 could be efficiently introduced into SIPI-KF; however, only a few exoconjugants (less than 5 colonies) grew out when pCL01 was introduced (Fig. S14c). The results clearly demonstrated that the toxicity of the yeast element is the key bottleneck hampering the introduction of pCL01-milbe into SIPI-KF. We observed similar toxic

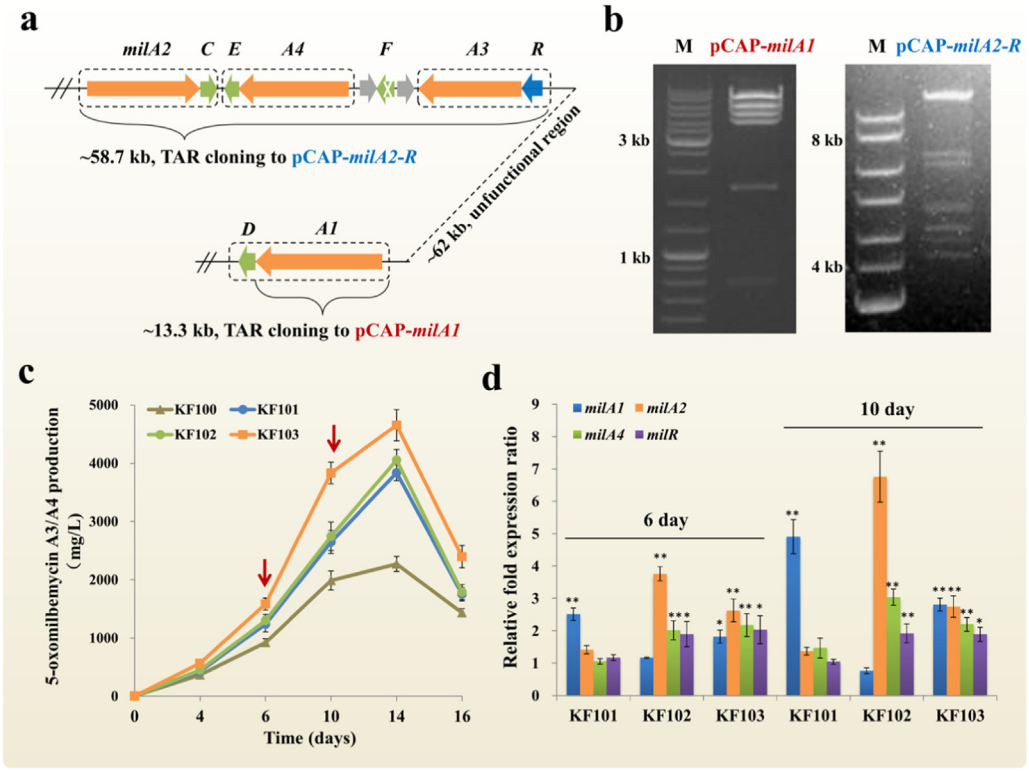

Fig. 5. Chromosomal integration of two separate parts of the 5-oxomilbemycin biosynthetic gene cluster (BGC) in *S. hygroscopicus* SIPI-KF. (a) Genetic organization of 5-oxomilbemycin BGC. The 5-oxomilbemycin biosynthetic genes (from *milA1* to *milA4*) and regulatory gene (*milR2*) are indicated with yellow and blue arrows, respectively. The tailoring enzyme genes (from *milC* to *milE*) are indicated with green arrows. Notably, the tailoring enzyme gene *milF* was deleted in *S. hygroscopicus* SIPI-KF. Grey arrows represent genes of unknown function. Interestingly, there is a large ~62 kb insertion between the genes *milA1* and *milR*. Therefore, two discrete parts of the 5-oxomilbemycin BGC were first captured into the cloning vector pCAP01a using Cas9-assisted TAR cloning method, generating the plasmids pCAP-*milA1* and pCAP-*milA2-R*, respectively. (b) Restriction analysis of the plasmids pCAP-*milA1* and pCAP-*milA2-R*. The expected band sizes of pCAP-*milA1* double-digested with *Xho*I and *Eco*RV were 7173, 5180, 4519, 3732, 1554, 738 and 156 bp. The 156-bp band ran off the agarose gel. The expected band sizes of pCAP-*milA2-R* digested with *Xho*I were 13,350, 12,698, 6253, 6075, 4392, 4214, 3843, 3812, 3641, 3627, 3498, 1067, 987 and 227 bp. The 1067-, 987- and 227-bp bands ran off the agarose gel. (c) Fermentation analysis of *S. hygroscopicus* SIPI-KF-derived strains with chromosomal integration of the *milA1* gene and/or the *milA2-R* gene cluster. The engineered strain KF100 (SIPI-KF/pCAP01a) was used as the negative control. The engineered strains KF101 (SIPI-KF/pCAP-*milA1*), KF102 (SIPI-KF/pCAP-*milA2-R*) and KF103 (SIPI-KF/pCAP-*milA2-R*/pRT802-*milA1*), which contain one extra copy of *milA1*, one extra copy of *milA2-R* and both *milA1* and *milA2-R*, were constructed, respectively. Fermentation samples were collected at five time points, and the experiments were performed in triplicate, $*p < 0.05$. (d) Transcriptional analysis of four selected 5-oxomilbemycin biosynthetic genes. Fermentation samples for RNA isolation were collected at 6 and 10 days. The relative transcription levels of the tested genes were normalized to that of *hrdB*. The relative fold changes in the expression of each gene (KF101–103 versus KF100) were determined using the $2^{-\Delta\Delta Ct}$ method. Data are analysed by *t*-test. Error bars indicate the standard deviations from three independent biological replicates, $*p < 0.05$.

effect when the pCL01 vector (containing the yeast element) was introduced into *S. pristinaespiralis* HCCB10218 by conjugal transfer. However, interestingly, no obvious toxic effect was observed when the same vector was transferred into *S. coelicolor* M145 or *Streptomyces albus* J1074 (Fig. S15). The detailed mechanism for the distinct toxic effects of the yeast element in different *Streptomyces* strains remains to be investigated in the future. From a practical perspective, the yeast element was removed, and the *ΦC31-acc(3)IV* IR cassette in pCL01-milbe was replaced by the SV1-*aphII* cassette from pLS2 and the SV1-R4-*aphII* IR cassette from pLSR2 using the CGE method, generating two plasmids with the *aphII* resistant marker, BAC-milbe-S (containing one integration module) and BAC-milbe-SR (containing two integration modules), respectively. Next, the *ΦC31-acc(3)IV* cassette from pLC1, the *ΦC31-ΦBT1-acc(3)IV* cassette from pLCB1, the *ΦC31-TG1-acc(3)IV* cassette from pLCT1 and the *ΦC31-ΦBT1-TG1-acc(3)IV* cassette from pLCBT1 were used to replace the SV1-*aphII* cassette in BAC-milbe-S, generating four plasmids with the *acc(3)IV* resistant marker, BAC-milbe-C, BAC-milbe-CB, BAC-milbe-CT and BAC-milbe-CBT, respectively. After verification by restriction analysis (Fig. 6b), the above four BAC plasmids were introduced into *S. hygroscopicus* SIPI-KF by conjugal transfer. We observed that when the yeast element was removed, the plasmids BAC-milbe-C and BAC-milbe-CB could be efficiently integrated into SIPI-KF (Fig. S14d), thus generating the engineered strains SIPI-KF/BAC-milbe-C (KF201, containing one extra copy of 5-oxomibemycin BGC) and SIPI-KF/BAC-milbe-CB (KF202, containing two extra copies of 5-oxomibemycin BGC), respectively. However, neither BAC-milbe-CT nor BAC-milbe-CBT could be introduced into SIPI-KF. The two-copy integration efficiency was 35% (3/10 + 4/10) when BAC-milbe-CB was introduced into SIPI-KF (Fig. S16a). As the negative control, the plasmid BAC-F15 was also integrated into SIPI-KF to generate KF200. Fermentation analysis showed that the introduction of BAC-milbe-C (KF201) and BAC-milbe-CB (KF202) led to maximum increases in 5-oxomilbemycin biosynthesis of 98% (from 2228 to 4415 mg/L) and 151% (from 2228 to 5592 mg/L), respectively (Fig. 6c).

Then, we attempted to realize four-copy amplification of the entire 5-oxomilbemycin BGC by two-round iterative integration to further enhance 5-oxomilbemycin production. Two plasmids with the *aphII* resistant marker, BAC-milbe-S and BAC-milbe-SR, were integrated into the strain KF202, generating the engineered strains KF203 (SIPI-KF/BAC-milbe-CB/BAC-milbe-S, containing three extra copies of 5-oxomibemycin BGC) and KF204 (SIPI-KF/BAC-milbe-CB/ BAC-milbe-SR, containing four extra copies of 5-oxomibemycin BGC). The two-copy integration efficiency was 35% (4/10 + 3/10) when the plasmid BAC-milbe-SR was introduced (Fig. S16b). Phenotypic analysis showed that KF201-KF204 had no obvious growth difference relative to KF200 (Fig. S17). Fermentation analysis showed that the maximum 5-oxomilbemycin titer of KF203 was further improved by 14% (from 5592 to 6368 mg/L) relative to that of KF202 (Fig. 6c). However, the 5-oxomilbemycin titer of KF204 was lower than that of KF203, possibly due to the metabolic burden from the simultaneous four-copy overexpression of the 5-oxomilibemycin BGC. Finally, chromosomal integration of the 5-oxomilbemycin BGC into the three native *attB* sites in the engineered strain KF203 was further verified by qPCR analysis of the copy numbers of four structural genes (*milA1-milA4*), as shown in Fig. S18a.

Subsequently, to investigate the effects of multi-copy integration of the entire BGC on 5-oxomilbemycin production at the transcriptional

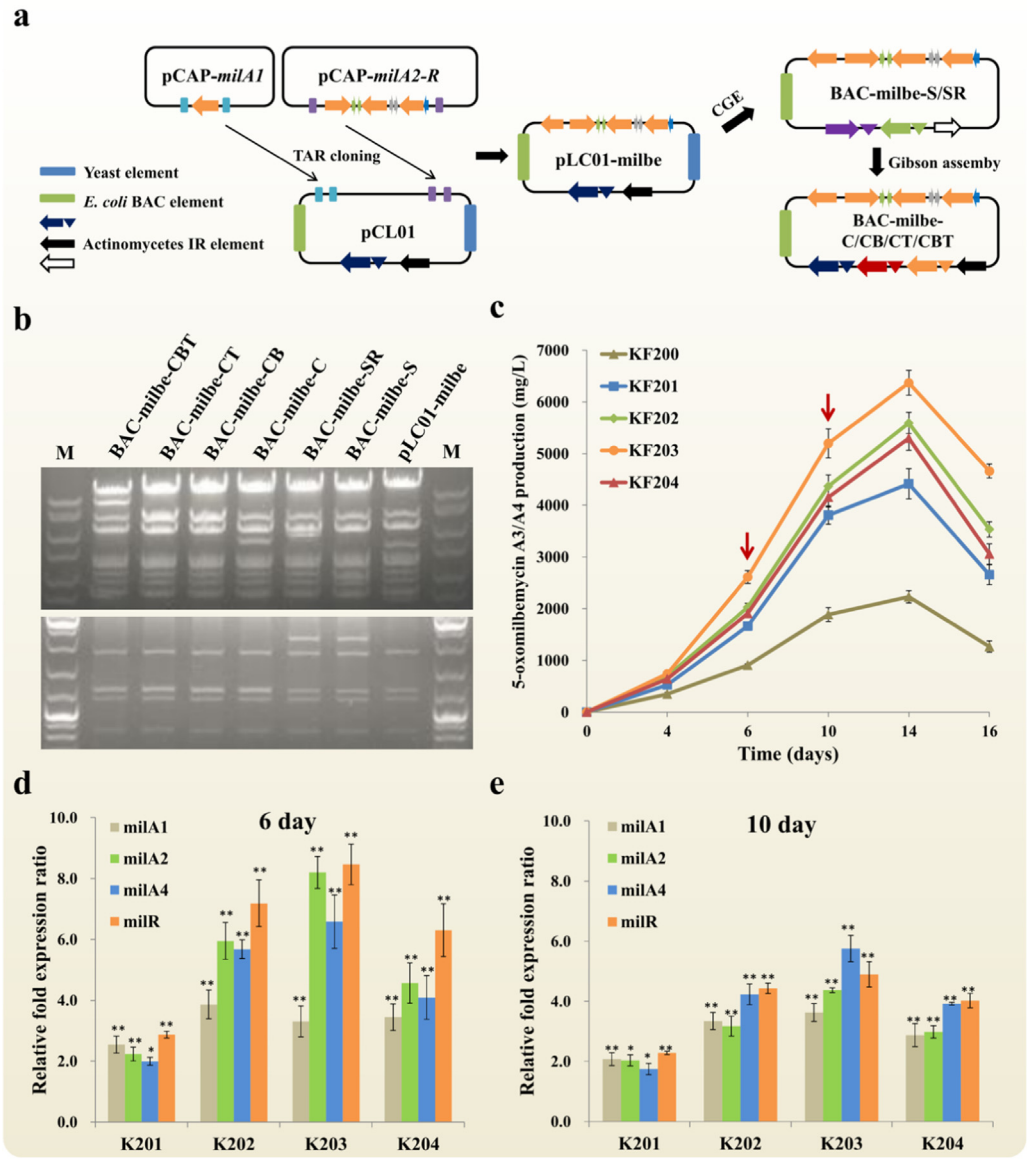

Fig. 6. aMSGE method for enhanced biosynthesis of 5-oxomilbemycin in *S. hygroscopicus* SIPI-KF. (a) Assembly and in vitro editing of the entire 5-oxomilbemycin BGC. The gene *milA1* and the gene cluster *milA2-R* were iteratively ligated into the captured vector pCL01 using TAR cloning, thus generating the plasmid pLC01-milbe. Then, the CGE method was employed to remove the yeast element (replication sequence and auxotrophic marker) and add the *aphII*-marked integration/resistance (IR) cassettes into pCL01-milbe, generating the plasmids BAC-milbe-S and BAC-milbe-SR. Finally, *Nsi*I was used to remove the SV1-*aphII* cassette from BAC-milbe-S, and Gibson assembly method was used to add a series of *acc(3)IV*-marked IR cassettes, generating BAC-milbe-C, BAC-milbe-CB, BAC-milbe-CT and BAC-milbe-CBT. (b) Restriction analysis of the entire 5-oxomilbemycin BGC with a series of different combinations of multi-copy integration systems. The expected band sizes of the plasmid pCL01-milbe digested with *Xho*I were 13,350, 12,698, 7173, 6383, 6253, 5009, 4392, 4353, 4214, 3812, 3641, 3627, 3498, 3377, 1554,1067, 987, 738, 272 and 156 bp. The 272- and 156-bp bands ran off the agarose gel. Regarding the expected bands after digestion of the plasmid BAC-milbe-S, the 5009-bp band disappeared, and the 3938- and 2023-bp bands appeared. For the expected bands after digestion of the plasmid BAC-milbe-SR, the 5009-bp band disappeared, and the 5889- and 2023-bp bands appeared. For the expected bands after digestion of the plasmid BAC-milbe-C, the 5009-bp band disappeared, and the 5427- and 1103-bp bands appeared. For the expected bands after digestion of the plasmid BAC-milbe-CB, the 5009-bp band disappeared, and the 7417- and 1103-bp bands appeared. For the expected bands after digestion of the plasmid BAC-milbe-CT, the 5009-bp band disappeared, and the 7173-and 1103-bp bands appeared. For the expected bands after digestion of the plasmid BAC-milbe-CBT, the 5009-bp band disappeared, and the 9577- and 1103-bp bands appeared. (c) Fermentation analysis of the engineered strains with chromosomal integration of different copies (from one to four) of the entire 5-oxomilbemycin BGC. The engineered strain KF200 (SIPI-KF/BAC-F15) was used as the negative control. Fermentation samples were collected at five time points, and the experiments were performed in triplicate. (d and e) Transcriptional analysis of four selected 5-oxomilbemycin biosynthetic genes. Fermentation samples for RNA isolation were collected at 6 and 10 days. The relative transcription levels of the tested genes were normalized to that of the *hrdB* gene. The relative fold-changes in the expression of each gene (KF201-KF204 versus KF200) were determined using the $2^{-\Delta\Delta Ct}$ method. Data are analysed by *t*-test. Error bars indicate the standard deviations from three independent biological replicates, $^{*}p < 0.05$.

level, we compared the transcription of four 5-oxomilbemycin biosynthetic genes (*milA1*, *milA2*, *milA4* and *milR*) in KF201-KF204 with that of KF100 by qRT-PCR analysis. Except for transcription in KF204, the mRNA levels of the four tested genes were significantly enhanced along with the increases of BGC copy numbers in KF201-KF203 (Fig. 6d and e). Finally, to further examine the genetic stability of the engineered strains constructed by aMSGE, the engineered strain KF203 were cultured over five generations in the absence of antibiotic selection. Fermentation analysis showed that the first (G1), third (G3) and fifth (G5) generations of KF203 were capable of producing similar 5-oxomilbemycin titers as that of the starting strain (Fig. S18b). The results clearly demonstrated that stable amplification of the entire 5-oxomilbemycin BGC using the aMSGE method is an efficient strategy to construct engineered strains producing high amounts of 5-oxomilbemycin.

3. Discussion

Effective tools to optimize the biosynthetic performance of target products in microbial fermentation systems are essential to achieve cost-efficient industrial production, and the development of such tools remains a long-standing challenge (Lee and Kim, 2015; Nielsen and Keasling, 2016). Indeed, a number of metabolic engineering efforts, such as varying promoter strength, enhancing antibiotic resistance and optimizing regulatory networks (Cho et al., 2015; Keasling, 2012), have been proven to be very useful strategies for accelerating strain improvement. However, in some cases where the copy number of the biosynthetic pathway limits enzyme production, one can amplify target

pathways in the host genome to increase the copy number (Tyo et al., 2009). As a powerful enabling technology, stable amplification of biosynthetic genes/pathways has broad applications for strain development in a wide variety of industrial microbes (Li et al., 2017a; Liu et al., 2017; Ou et al., 2018). However, it is still a daunting task to introduce large metabolic pathways into different chromosomal loci for stable expression in a simple process. In this study, we describe a methodology and corresponding toolkit that allows for rapid, multi-copy integration of biosynthetic gene clusters for the development of pharmaceutically active natural products in actinomycetes. A modular multi-integration plasmid library was provided for high-efficiency genomic integration of target genes or pathways with up to four copies in a single step (Table 1). Compared with previously reported methods, such as MSGE and ZouA-mediated tandem amplification (Li et al., 2017b; Murakami et al., 2011), the aMSGE method does not require the introduction of any modifications into host genomes before gene or pathway integration. Therefore, this novel technique can significantly simplify and accelerate genetic manipulation efforts and is suitable for multiplex site-specific genome engineering to enhance the biosynthesis of important naturally derived drugs in the genetically tractable and intractable industrial actinomycetes (Barka et al., 2016; Weber et al., 2015).

Thus far, we were able to efficiently integrate three genes, *accA2BE*, into the model strain *S. coelicolor* with three copies in a single step, leading to a 4.6-fold increase in actinorhodin production. Furthermore, using this plug-and-play toolkit, the large, full 5-oxomilbemycin BGC (~72 kb) was integrated into the industrial strain *S. hygroscopicus* with three copies, leading to a 1.9-fold increase in 5-oxomilbemycin production (from 2.23 to 6.37 g/L). A main concern of the engineered strains generated by the aMSGE method is their genetically unstable owing to DNA homologous recombination between target genes or gene clusters (including both native and integrated ones). However, considering the discrete distribution of native *attB* sites, there locate many essential genes between these target genes or gene clusters. Therefore, if homologous recombination happen, bacteria will be killed. Actually, in our study, we showed that after five continuous passages without antibiotic selection, the fifth generation of the engineered strain KF203 still grew well (data not shown) and produced maximum 5-oxomilbemycin titers as that of the starting strain (Fig. S18b). It could be therefore concluded that the engineered strains obtained by the aMSGE method are genetically stable. Here, the engineered strains with four extra copies of the genes *accA2BE* or the 5-oxomilbemycin BGC were also constructed, but the titers of their corresponding end products were not further improved. This phenomenon might have two explanations. First, simultaneous overexpression of too many orthogonal integrases might be toxic to bacterial growth. Second, overexpression of biosynthetic genes or gene clusters with multiple copies might lead to severe metabolic burden due to protein overproduction or the accumulation of toxic end products. Similar phenomenon has also been observed when amplifying the pristinamycin II biosynthetic gene cluster in the industrial strain *S. pristinaespiralis* (Li et al., 2017b). Therefore, other metabolic engineering strategies, including ribosome engineering and optimization of regulatory networks (Liu et al., 2018; Weber et al., 2015; Zhang et al., 2016), should be combinatorially applicable to strain improvement for large-scale industrial fermentation.

In addition to the five orthogonal integration systems we used here, there are at least four other identified SSR systems in actinomycetes, including VWB, ΦJoe, ΦK38-1 and CBG73463 integration systems (Fig. S1). According to a systematic bioinformatics analysis, we found that there are at least four accessible integration systems among all the identified SSR systems in diverse actinomycetes species, including *Streptomyces*, *Actinoplanes*, *Saccharopolyspora*, *Amycolatopsis* and *Pseudonocardia* (Table 4). Therefore, the aMSGE method can synergize with synthetic biology and genome mining efforts to facilitate the biosynthesis of commercially useful products or the discovery of novel drug leads by amplification of target gene clusters in actinomycetes. More importantly, it is well known that site-specific recombination systems are widely distributed in a wide variety of industrial microbes, including *Escherichia coli*, *Bacillus*, *Pseudomonas*, *Lactococcus* and *Clostridium* (Fogg et al., 2014; St-Pierre et al., 2013; Stark, 2017; Yang et al., 2014). For example, there are at least five functional tyrosine integrases from phage 186, HK022, lambda, Φ80, and P21, which have already been applied to sequential integration of DNA constructs into their respective *attB* sites in *E. coli* (St-Pierre et al., 2013). Therefore, this principle of "multiple integrases-multiple *attB* sites" for the stable amplification of genes or metabolic pathways is readily applicable to a wide range of bacteria for enhanced synthesis of biochemicals, biopharmaceuticals and other value-added biomolecules.

4. Materials and methods

4.1. Strains, plasmids and growth conditions

The strains and plasmids used in this study are listed in Table S1. *S. coelicolor* M145 and its derivatives were grown on MS medium (g/L, soybean flour 20, mannitol 20, and agar 20) for spore preparation and intergeneric conjugal transfer (Kieser, 2000). RP (g/L, tryptone 5, yeast extract 5, valine 0.5, NaCl 2, KH_2PO_4 0.5, $MgSO_4{\cdot}7H_2O$ 1 and agar 20, pH 6.4) and MB (g/L, sucrose 4, skim milk 1, yeast extract 2, malt extract 5 and agar 20, pH 7.0–7.2) media were used for spore preparations from *Streptomyces pristinaespiralis* HCCB10218 and *Streptomyces hygroscopicus* SIPI-KF, respectively. M-Isp4 medium (g/L, soybean flour 5, mannitol 5, starch 5, tryptone 2, yeast extract 1, NaCl 1, $(NH_4)_2SO_4$ 2, K_2HPO_4 1, $CaCO_3$ 2, agar 20, and trace element solution 1 mL, pH 7.0–7.2) with 10 and 60 mM $MgCl_2$ was used for conjugal transfer from *E. coli* to *S. pristinaespiralis* and *S. hygroscopicus*, respectively (Li et al., 2018, 2015). Liquid MB and YEME media (g/L, yeast extract 3, peptone, 5, malt extract 3, glucose 10, sucrose 340 and $MgSO_4{\cdot}7H_2O$ 1.24) were used for genomic DNA isolation of *S. hygroscopicus* and *S. coelicolor*, respectively (Kieser, 2000; Li et al., 2018). All *Streptomyces* strains were cultivated at 30 °C.

Escherichia coli DH5α and EPI300 were used for DNA cloning. *E. coli* DH10B ET12567/pUB307, ET12567/pUZ8002 and S17-1 were used for conjugal transfer from *E. coli* to *Streptomyces*. The detailed intergeneric conjugation experiments were described in the supplemental materials. *E. coli* strains were grown at 37 °C in Luria-Bertani (LB) medium or on LB agar plates. Antibiotics (50 μg/mL ampicillin, apramycin, chloramphenicol and kanamycin) were added when necessary. *Saccharomyces cerevisiae* V6–48 was used for capturing and assembling the 5-oxomilbemycin BGC. *S. cerevisiae* strains were grown at 30 °C on solid or in liquid YPD medium (g/L, glucose 2, yeast extract 1, peptone 2 and adenine sulfate 0.08) (Lee et al., 2015).

4.2. Construction of the plug-and-play toolkit for multi-copy genomic integration of genes or pathways

The R4, SV1 and TG1 integration systems, each of which consists of an integrase gene and its corresponding *attP* site, were chemically synthesized. Then, the three elements were double-digested with *Bam*HI and *Sph*I and cloned into pSET152, thus generating the plasmids pLR4, pLSV1-T and pLTG1, respectively. Notably, the SV1 integrase gene is possibly cotranscribed with other genes, forming an operon in the genome of SV1 phage (Fayed et al., 2014). Therefore, to simplify plasmid construction, expression of the SV1 integrase (with its corresponding *attP* site) was designed to be under the control of the strong promoter *ermEp**. In contrast, the other four integrases were expressed by their native promoters containing corresponding *attP* sites. Using the plasmid pIB139 as a template, the strong promoter *ermEp** was obtained by PCR with the primers *ermEp**-fw/rev. The resulting DNA fragment was double-digested by *Bgl*II and *Nde*I and ligated into *Bam*HI/*Nde*I-digested pLSV1-T to generate the plasmid pLSV1. After testing the integration efficiencies of the above five plasmids in three different *Streptomyces*, we began to construct the plug-and-play toolkit

Table 4
Systematical analysis of eight site-specific integration systems' host range in the model and industrial actinomycetes.

Actinomycete strains	Products	ΦBT1-*attB*	ΦC31-*attB*	R4-*attB*	SV1-*attB*	TG1-*attB*	VWB-*attB*	ΦJoe-*attB*	ΦK38-1-*attB*
***Streptomyces coelicolor* A3(2)**	ACT/RED/CDA	Y	Y	Y	Y	Y	Y	N	Y
***Streptomyces albus* J1074**	NA	Y	Y	Y	N	Y	Y	Y	Y
***Streptomyces venezuelae* ATCC10172**	Chloramphenicol	Y	Y	Y	Y	Y	Y	Y	Y
***Streptomyces griseus* NBRC 13350**	Streptomycin	Y	Y	Y	Y	Y	Y	Y	Y
***Streptomyces avermitilis* MA-4680**	Avermectin	Y	Y	Y	Y	Y	Y	Y	Y
***Streptomyces pristinaespiralis* HCCB10218**	Pristinamycin	Y	Y	Y	Y	Y	Y	Y	Y
***Streptomyces globisorus* C-1027**	Lidamycin	Y	Y	Y	Y	Y	Y	Y	Y
***Streptomyces* jinggangensis 5008**	Validamycin	Y	Y	Y	Y	Y	Y	Y	Y
***Streptomyces rimosus* R6–500**	Oxytetracycline	Y	Y	N	Y	Y	N	Y	Y
***Streptomyces albus* DSM41398**	Salinomycin	Y	Y	Y	N	Y	N	Y	Y
***Streptomyces tsukubaensis* NRRL18488**	FK506	Y	Y	Y	N	Y	N	Y	Y
***Streptomyces natalensis* ATCC27448**	Natamycin	Y	Y	Y	N	Y	N	Y	Y
Streptomyces nodosus	Amphotericin	Y	Y	N	N	Y	Y	Y	Y
***Streptomyces fradiae* ATCC10745**	Tylosin	Y	Y	Y	N	Y	N	Y	Y
***Streptomyces roseosporus* NRRL15998**	Daptomycin	Y	Y	Y	Y	Y	N	Y	Y
***Streptomyces bingchenggenesis* BCW-1**	Milbemycin	Y	Y	Y	Y	Y	Y	Y	Y
Actinomycete Strains	**Products**	**ΦBT1-*attB***	**ΦC31-*attB***	**R4-*attB***	**SV1-*attB***	**TG1-*attB***	**VWB-*attB***	**ΦJoe-*attB***	**ΦK38–1-*attB***
***Streptomyces aureofaciens* ATCC10762**	Tetracycline	Y	Y	Y	Y	Y	N	Y	Y
Streptomyces kasugaensis	Kasugamycin	Y	Y	Y	Y	Y	N	Y	Y
***Streptomyces lincolnensis* NRRL2936**	Lincomycin	Y	Y	Y	Y	Y	Y	Y	Y
***Streptomyces clavuligerus* ATCC27064**	Clavulanic acid	Y	Y	Y	Y	Y	Y	Y	Y
***Streptomyces peucetius* ATCC27952**	Doxorubicin	Y	Y	N	N	Y	Y	Y	Y
***Actinoplanes sp.* SE50/110**	Acarbose	N	Y	Y	N	Y	N	Y	N
***Actinoplanes sp.* N902-109**	Rapamycin	N	Y	Y	N	Y	N	Y	N
***Saccharopolyspora erythraea* NRRL2338**	Erythromycin	N	N	Y	N	Y	Y	Y	N
***Saccharopolyspora spinosa* NRRL18395**	Spinosad	N	N	Y	N	Y	N	Y	N
***Amycolatopsis orientalis* HCCB10007**	Vancomycin	Y	Y	Y	N	Y	Y	N	N
***Amycolatopsis mediterranei* S699**	Rifamycin	Y	N	Y	N	Y	Y	N	N
***Pseudonocardia autotrophica* DSM 43083**	Polyene	N	Y	Y	N	Y	Y	Y	N

Note: ACT, RED and CDA represent three antibiotics, namely, actinorhodin, undecylprodiginines and calcium-dependent antibiotic, respectively. Y and N represent the existence and no existence of homologs (the identity of aa sequences is > 70%) in actinomycetes to the corresponding genes containing bacteriophage *attB* sites using the BlastP server, respectively. These genes are SCO4848 (ΦBT1), SCO3798 (ΦC31), SCO6196 (R4), SCO4383 (SV1), SCO3658 (TG1), tRNA_100038 (SCO) (VWB), SVEN_2383 (ΦJoe) and SCO1148 (ΦK38).

containing the single- or multi-integration modules by using the classical molecular cloning strategy. The construction workflow was shown in Fig. S19 and the detailed construction process was described in the Supplemental materials. The sequences of the plasmids containing single-or multi-integration modules could be retrieved from NCBI Genbank and the accession numbers were shown in Table 1.

4.3. Construction of a series of plasmids with multi-integration modules for acetyl-CoA carboxylase overexpression

The genes *accA2* and *accBE* (encoding acetyl-CoA carboxylase) were amplified from the *S. coelicolor* genomic DNA using the primers accA2-fw/rev and accBE-fw/rev, respectively. The two DNA fragments were ligated together by overlapping PCR using the primers accA2-fw/accBE-rev. After treatment with *Eco*RI and *Nde*I, the DNA fragment was cloned into pIB139 to generate pIB-A2BE. Then, using pIB-A2BE as the template, the *accA2BE* cassette were obtained by PCR using the primers accA2-fw/accBE-rev and recombined into *Pac*I-digested pLC1, pLCB1 pLCBR1 and pLCBRS1, thus generating the plasmids pLC1-A2BE (containing the ΦC31 integration system), pLCB1-A2BE (containing the ΦC31 and ΦBT1 integration systems), pLCBR1-A2BE (containing the ΦC31, ΦBT1 and R4 integration systems) and pLCBRS1-A2BE (containing the ΦC31, ΦBT1, R4 and SV1 integration systems), respectively. The primers used are listed in Table S2 in the Supplementary materials.

4.4. Cloning of the 5-oxomilbemycin BGC by CRISPR-assisted yeast transformation-associated recombination (TAR)

4.4.1. TAR cloning of the two separate parts of 5-oxomilbemycin BGC

The capture vector pCAP01a, derived from the original capture vector pCAP01 (Yamanaka et al., 2014), was used to clone the two parts of 5-oxomilbemycin BGC. The construction process of the vector pCAP01a was described in the Supplementary materials. Then, two recombinant plasmids, pCAP-*milA1*-HR and pCAP-*milA2-R*-HR, were constructed for the capture of *milA1* and the partial 5-oxomilbemycin gene cluster *milA2-R*, respectively. Briefly, two homologous arms (1804 and 1826 bp) flanking the gene *milA1* were amplified from SIPI-KF genomic DNA with the respective primer pairs, milA1-up-fw/rev and milA1-down-fw/rev. Then, the two PCR products were ligated together by overlapping PCR using the primers milA1-up-fw/milA1-down-rev and cloned into pCAP01a to generate the capture plasmid pCAP-*milA1*-HR. Similarly, the capture plasmid pCAP-*milA2-R*-HR was generated. Then, CRISPR-assisted TAR cloning method was used to capture the two separate parts of the 5-oxomilbemycin BGC into the plasmids pCAP-*milA1*-HR and pCAP-*milA2-R*-HR, thus generating the plasmids pCAP-*milA1* and pCAP-*milA2-R*, respectively (Lee et al., 2015). The cloning workflow was shown in Fig. S20 and the detailed construction process was described in the Supplemental materials. Finally, the gene *milA1* was obtained from pCAP-*milA1* by digestion with *Spe*I and *Xba*I and cloned into pRT802 to generate the plasmid pRT802-*milA1* (data not shown).

4.4.2. TAR cloning of the entire 5-oxomilbemycin BGC

To clone the large, entire 5-oxomilbemycin BGC, a new cloning vector pCL01 was constructed based on the copy-control plasmid pCC1BAC (Fig. S14a). We first cloned the *milA1* gene, and then the gene cluster *milA2-R* was further captured using the recombinant plasmid with *milA1* as the capture vector using TAR cloning method. Finally, the plasmid pCL01-milbe was obtained, which contains the entire 5-oxomilbemycin BGC, followed by verification using sequencing as well as restriction analysis. The cloning workflow was shown in Fig. S20 and the detailed construction process was described in the Supplemental materials.

4.5. Construction of pCL01-milbe-derived plasmids containing different multi-integration systems

Based on pCL01-milbe, we generated two plasmids, namely, BAC-milbe-S and BAC-milbe-SR, in which both the yeast element (ARSH4/CEN6-TRP1) and the *Φ*C31-*acc(3)IV* IR cassette were removed and replaced by the SV1-*aphII* and SV1-R4-*aphII* cassettes, respectively, using the CGE method (Li et al., 2017b). The cloning workflow was shown in Fig. 6a. Briefly, pCL01-milbe was digested with Cas9 guided by two sgRNAs (including sgRNA-ARSH4/CEN6-TPR1-up and sgRNA-*Φ*C31-int-down) for 4 h at 37 °C, and the linearized plasmid was recovered by ethanol precipitation. The SV1-*aphII* and SV1-R4-*aphII* cassettes were amplified from pLS2 and pLSR2 using the primer pairs S-aphII-fw/rev and SR-aphII-fw/rev, respectively. Then, the SV1-*aphII* and SV1-R4-*aphII* cassettes were individually recombined into the Cas9-digested plasmid by the Gibson assembly method (Li et al., 2017b), thus generating BAC-milbe-S and BAC-milbe-SR.

Based on BAC-milbe-S, four pCL01-milbe-derived plasmids with the *acc(3)IV* resistance marker, including BAC-milbe-C, BAC-milbe-CB, BAC-milbe-CT and BAC-milbe-CBT, which each contain one to three different integration systems, were constructed as follows. Briefly, the plasmid BAC-milbe-S was digested with *Nsi*I to remove the SV1-*aphII* cassette, resulting in the linearized DNA fragment BAC-milbe-L, which was recovered by ethanol precipitation. The *Φ*C31-*acc(3)IV*, *Φ*C31-*Φ*BT1-*acc(3)IV*, *Φ*C31-TG1-*acc(3)IV* and *Φ*C31-*Φ*BT1-TG1-*acc(3)IV* IR cassettes were obtained from the plasmids pLC1, pLCB1 pLCT1 and pLCBT1, respectively, by digestion with *Spe*I. Then, the corresponding IR cassettes described above were recombined into BAC-milbe-L to generate BAC-milbe-C, BAC-milbe-CB, BAC-milbe-CT and BAC-milbe-CBT by Gibson assembly (Gibson et al., 2009).

4.6. Demonstration of the plug-and-play integration toolkit in S. coelicolor and S. pristinaespiralis

A series of modular plasmids (totally 18 plasmids) containing two integration systems, three integration systems and four integration systems were individually introduced into M145 by conjugal transfer, thus generating the corresponding engineered strains. To test four-copy iterative integration, three plasmids with the *acc(3)IV* resistance marker, including pLBT1, pLCB1 and pLCT1, were individually introduced into M145/pLSR2 (with kanamycin resistance) to generate three strains with different combinations of four integration systems (M145/pLSR2-BT1, M145/pLSR2-CB1 and M145/pLSR2-CT1). The plasmid pLCT1 was introduced into M145/pLBR2 and M145/pLBS2 to generate M145/pLBR2-CT1 and M145/pLBS2-CT1, respectively. The primer pairs ID-oriT-fw/ID-*Φ*C31-attB-rev(SCO) and ID-oriT-fw/ID-*Φ*BT1-attB-rev(SCO) were used to track the successful integration of the *Φ*C31 integration system into the plasmids pLCB1/pLCT1 and the *Φ*BT1 integration system into the plasmids pLBT1/pLBR2/pLBS2 The primer pair ID-*Φ*C31-fw/ID-*Φ*BT1-attB-rev(SCO) was used to track the successful integration of the plasmid pLCB1 and its derived plasmids into *Φ*BT1 *attB* sites. Primer pairs ID-R4-fw/ID-R4-attB-rev(SCO), ID-SV1-fw/ID-SV1-attB-rev(SCO) and ID-TG1-fw/ID-TG1-attB-rev(SCO) were used to track the successful integration of the R4, SV1 and TG1 integration systems into corresponding *attB* sites. It is worth noting that plasmids with the *aphII* resistance marker, including pLS2, pLSR2, pLSRB2 and pLSRBC2, were introduced into *S. coelicolor* using triparental conjugal transfer (Flett et al., 1997). The *aphII*-marked plasmids were first transferred into DH10B, which served as joint donor strains with ET12567/pUB307.

Similarly, the primer pairs ID-oriT-fw/ID-*Φ*C31-attB-rev(SPR) and ID-oriT-fw/ID-*Φ*BT1-attB-rev(SPR) were used to track the successful integration of the *Φ*C31 integration system of the plasmids pLCB1/pLCT1 and the *Φ*BT1 integration system of the plasmids pLBT1/pLBR2/pLBS2. Then, the primer pair ID-*Φ*C31-fw/ID-*Φ*BT1-attB-rev(SPR) was used to track the successful integration of the plasmid pLCB1 and its derived plasmids into native *Φ*BT1 *attB* sites. ID-R4-fw/ID-R4-attB-rev (SPR), ID-SV1-fw/ID-SV1-attB-rev(SPR) and ID-TG1-fw/ID-TG1-attB-rev(SPR) were used to track the successful integration of the R4, SV1 and TG1 integration systems into corresponding native *attB* sites.

4.7. Construction of S. coelicolor mutants with chromosomal integration of different copies of accA2BE encoding the acetyl-CoA carboxylase

Recombinant plasmids, including pIB-A2BE, pLC1-A2BE, pLCB1-A2BE, pLCBR1-A2BE and pLCBRS1-A2BE, and the empty plasmid pIB139 were individually introduced into M145 by conjugal transfer, thus generating the corresponding engineered strains. The primer pairs ID-oriT-fw/ID-*Φ*C31-attB-rev(SCO), ID-*Φ*C31-fw/ID-*Φ*BT1-attB-rev (SCO), ID-R4-fw/ID-R4-attB-rev(SCO), ID-SV1-fw/ID-SV1-attB-rev (SCO) and ID-TG1-fw/ID-TG1-attB-rev(SCO) were used to track the successful integration of the above plasmids into corresponding *attB* sites by PCR analysis. In each experiment, ten exconjugants were randomly picked to determine the integration efficiency.

4.8. Construction of S. hygroscopicus mutants with chromosomal integration of different copies of the 5-oxomilbemycin BGC

The empty plasmid pCAP01a and two recombinant plasmids, including pCAP-*milA1* and pCAP-*milA2-R*, were introduced into *S. hygroscopicus* SIPI-KF, thus generating the engineered strains KF100, KF101 and KF102, respectively. Then, the plasmid pRT802-*milA1* (containing the *Φ*BT1-*aphII* IR cassette) was introduced into KF102 to generate KF103. The plasmids BAC-F15, BAC-milbe-C and BAC-milbe-CB were introduced into SIPI-KF to generate the engineered strains KF200, KF201 and KF202, respectively. BAC-milbe-S or BAC-milbe-SR was integrated into KF202, generating the engineered strains KF203 and KF204, respectively. The primer pairs ID-oriT-fw/ID-*Φ*C31-attB-rev (SBIN), ID-*Φ*C31-fw/ID-*Φ*BT1-attB-rev(SBIN), ID-R4-fw/ID-R4-attB-rev (SBIN) and ID-SV1-fw/ID-SV1-attB-rev(SBIN) were used to track the successful integration of the above plasmids into corresponding *attB* sites. The primers used are listed in Table S2 in the Supplementary materials.

4.9. Fermentation of S. hygroscopicus and HPLC analysis of 5-oxomilbemycin A3/A4 production

For 5-oxomilbemycin A3/A4 production, *S. hygroscopicus* strains were first grown on solid MB medium at 30 °C for 6–7 days and then inoculated into 25 mL of seed medium (g/L, sucrose 20, meat peptone 2.5, yeast extract 5 and K_2HPO_4 0.1, pH 7.2) in 250-mL Erlenmeyer flasks on an orbital shaker (240 rpm). After incubation at 28 °C for 24–28 h, 1 mL of pre-culture was inoculated into 25 mL of fermentation medium (g/L, sucrose 120, cotton seed meal 5, soybean flour 5, K_2HPO_4 0.5, $FeSO_4{\cdot}7H_2O$ 0.1 $ZnSO_4{\cdot}7H_2O$ 0.01, $CuSO_4{\cdot}7H_2O$ 0.05 and $CaCO_3$ 3) in 250-mL Erlenmeyer flasks. The pH of the fermentation medium was adjusted to 7.2 prior to the addition of $CaCO_3$.

Fermentation samples (1 mL) were collected at five time points (4, 6, 10, 14 and 16 days) and extracted with the same volume of ethanol for 1–2 h. Subsequently, the mixtures were centrifuged at 12,000 rpm for 10 min, and the supernatants (ethanol extracts) were directly analysed by HPLC (1100 series, Agilent) using a 4.6 × 150 mm Hypersil C18 column (Agilent). For HPLC detection, a mixture of acetonitrile/H_2O (73:27, v/v) was used as the mobile phase, with a flow rate of 1.2 mL/min and a retention time of 14 min for 5-oximilbemycin A3 and 20 min for 5-oximilbemycin A4. The eluates were monitored at 240 nm, and the column temperature was set at 30 °C.

4.10. RNA preparation and quantitative real-time RT-PCR (RT-qPCR)

RNA preparation and RT-qPCR analysis were performed as previously described (R. Wang et al., 2013). The primers used are listed in

Table S2. Cultures of *S. hygroscopicus* grown in fermentation medium were harvested for RNA preparation at 6 and 10 days. RT-qPCR analysis was performed with the MyiQ2 two-color real-time PCR detection system (Bio-Rad, USA) by using iQ™ SYBR Green Supermix (Bio-Rad, USA). Reactions were conducted in triplicate for each transcript and repeated with three independent samples. The *hrdB* gene (*SBI_16115)*, encoding the principal sigma factor, was used as an internal control. The relative expression levels of tested genes were normalized to those of *hrdB*. Relative fold-changes in the transcription of each gene were determined using the $2^{-\Delta\Delta Ct}$ method (Livak and Schmittgen, 2001). Error bars indicate the standard deviations from three independent biological replicates.

Acknowledgements

This work was supported by the National Natural Science Foundation of China (31430004, 31630003, 31570072 and 31770088), the National Postdoctoral Program for Innovative Talents (BX201700265), the China Postdoctoral Science Foundation (2017M621545), the Science and Technology Commission of Shanghai Municipality (18ZR1446700 and 16490712100), the National Mega-project for Innovative Drugs (2018ZX09711001-006-012) and the Derivative Bank of Chinese Biological Resources, CAS (ZSYS-016).

Appendix A. Supporting information

Supplementary data associated with this article can be found in the online version at doi:10.1016/j.ymben.2018.12.001.

References

Baltz, R.H., 2012. *Streptomyces* temperate bacteriophage integration systems for stable genetic engineering of actinomycetes (and other organisms). J. Ind. Microbiol. Biotechnol. 39, 661–672.
Barka, E.A., Vatsa, P., Sanchez, L., Gaveau-Vaillant, N., Jacquard, C., Klenk, H.P., Clement, C., Ouhdouch, Y., van Wezel, G.P., 2016. Taxonomy, physiology, and natural products of actinobacteria. Microbiol. Mol. Biol. Rev. 80, 1–43.
Bonnet, J., Yin, P., Ortiz, M.E., Subsoontorn, P., Endy, D., 2013. Amplifying genetic logic gates. Science 340, 599–603.
Bowman, D.D., Reinemeyer, C.R., Wiseman, S., Snyder, D.E., 2014. Efficacy of milbemycin oxime in combination with spinosad in the treatment of larval and immature adult stages of *Ancylostoma caninum* and *Toxocara canis* in experimentally infected dogs. Vet. Parasitol. 205, 134–139.
Butler, M.S., Robertson, A.A.B., Cooper, M.A., 2014. Natural product and natural product derived drugs in clinical trials. Nat. Prod. Rep. 31, 1612–1661.
Chater, K.F., Carter, A.T., 1979. New, wide host-Range, temperate bacteriophage-(R4) of *Streptomyces* and its interaction with some restriction-modification systems. J. Gen. Microbiol. 115, 431–442.
Cho, C., Choi, S.Y., Luo, Z.W., Lee, S.Y., 2015. Recent advances in microbial production of fuels and chemicals using tools and strategies of systems metabolic engineering. Biotechnol. Adv. 33, 1455–1466.
Choi, K.R., Lee, S.Y., 2016. CRISPR technologies for bacterial systems: current achievements and future directions. Biotechnol. Adv. 34, 1180–1209.
Colloms, S.D., Merrick, C.A., Olorunniji, F.J., Stark, W.M., Smith, M.C.M., Osbourn, A., Keasling, J.D., Rosser, S.J., 2014. Rapid metabolic pathway assembly and modification using serine integrase site-specific recombination. Nucleic Acids Res. 42, e23.
Court, D.L., Sawitzke, J.A., Thomason, L.C., 2002. Genetic engineering using homologous recombination. Annu. Rev. Genet. 36, 361–388.
Donohoue, P.D., Barrangou, R., May, A.P., 2018. Advances in industrial biotechnology using CRISPR-Cas systems. Trends Biotechnol. 36, 134–146.
Fayed, B., Younger, E., Taylor, G., Smith, M.C.M., 2014. A novel *Streptomyces* spp. integration vector derived from the *S. venezuelae* phage, SV1. BMC Biotechnol. 14, 51.
Flett, F., Mersinias, V., Smith, C.P., 1997. High efficiency intergeneric conjugal transfer of plasmid DNA from *Escherichia coli* to methyl DNA-restricting streptomycetes. FEMS Microbiol. Lett. 155, 223–229.
Fogg, P.C.M., Colloms, S., Rosser, S., Stark, M., Smith, M.C.M., 2014. New applications for phage integrases. J. Mol. Biol. 426, 2703–2716.
Fogg, P.C.M., Haley, J.A., Stark, W.M., Smith, M.C.M., 2017. Genome integration and excision by a new *Streptomyces* bacteriophage, *Φ*Joe. Appl. Environ. Microbiol. 83, e02767–16.
Genilloud, O., 2017. Actinomycetes: still a source of novel antibiotics. Nat. Prod. Rep. 34, 1203–1232.
Gibson, D.G., Young, L., Chuang, R.Y., Venter, J.C., Hutchison, C.A., Smith, H.O., 2009. Enzymatic assembly of DNA molecules up to several hundred kilobases. Nat. Methods 6, 343–U41.
Gregory, M.A., Till, R., Smith, M.C.M., 2003. Integration site for *streptomyces* phage phiBT1 and development of site-specific integrating vectors. J. Bacteriol. 185, 5320–5323.
Grindley, N.D.F., Whiteson, K.L., Rice, P.A., 2006. Mechanisms of site-specific recombination. Annu. Rev. Biochem. 75, 567–605.
Haginaka, K., Asamizu, S., Ozaki, T., Igarashi, Y., Furumai, T., Onaka, H., 2014. Genetic approaches to generate hyper-producing strains of goadsporin: the relationships between productivity and gene duplication in secondary metabolite biosynthesis. Biosci. Biotechnol. Biochem. 78, 394–399.
Keasling, J.D., 2012. Synthetic biology and the development of tools for metabolic engineering. Metab. Eng. 14, 189–195.
Kieser, T., Bibb, M.J., Butter, M.J., Chater, K.F., Hopwood, D.A., 2000. Practical *Streptomyces* Genetics. The John Innes Foundation, Norwich, United Kingdom.
Kim, J.H., Feng, Z.Y., Bauer, J.D., Kallifidas, D., Calle, P.Y., Brady, S.F., 2010. Cloning large natural product gene clusters from the environment: piecing environmental DNA gene clusters back together with TAR. Biopolymers 93, 833–844.
Lee, N.C., Larionov, V., Kouprina, N., 2015. Highly efficient CRISPR/Cas9-mediated TAR cloning of genes and chromosomal loci from complex genomes in yeast. Nucleic Acids Res. 43, e55.
Lee, S.Y., Kim, H.U., 2015. Systems strategies for developing industrial microbial strains. Nat. Biotechnol. 33, 1061–1072.
Li, L., Jiang, W.H., Lu, Y.H., 2017a. New strategies and approaches for engineering biosynthetic gene clusters of microbial natural products. Biotechnol. Adv. 35, 936–949.
Li, L., Wei, K.K., Zheng, G.S., Liu, X.C., Chen, S.X., Jiang, W.H., Lu, Y.H., 2018. CRISPR-Cpf1 assisted multiplex genome editing and transcriptional repression in *Streptomyces*. Appl. Environ. Microbiol. 84, e00827–18.
Li, L., Zhao, Y.W., Ruan, L.J., Yang, S., Ge, M., Jiang, W.H., Lu, Y.H., 2015. A stepwise increase in pristinamycin II biosynthesis by *Streptomyces pristinaespiralis* through combinatorial metabolic engineering. Metab. Eng. 29, 12–25.
Li, L., Zheng, G.S., Chen, J., Ge, M., Jiang, W.H., Lu, Y.H., 2017b. Multiplexed site-specific genome engineering for overproducing bioactive secondary metabolites in actinomycetes. Metab. Eng. 40, 80–92.
Liu, H., Jiang, H., Haltli, B., Kulowski, K., Muszynska, E., Feng, X.D., Summers, M., Young, M., Graziani, E., Koehn, F., Carter, G.T., He, M., 2009. Rapid cloning and heterologous expression of the meridamycin biosynthetic gene cluster using a versatile *Escherichia coli-streptomyces* artificial chromosome vector, pSBAC. J. Nat. Prod. 72, 389–395.
Liu, R., Deng, Z.X., Liu, T.G., 2018. *Streptomyces* species: ideal chassis for natural product discovery and overproduction. Metab. Eng. https://doi.org/10.1016/j.ymben.2018.05.015.
Liu, Z.H., Liang, Y.Y., Ang, E.L., Zhao, H.M., 2017. A new era of genome integration-simply cut and paste!. ACS Synth. Biol. 6, 601–609.
Livak, K.J., Schmittgen, T.D., 2001. Analysis of relative gene expression data using real-time quantitative PCR and the 2(T)(-Delta Delta C) method. Methods 25, 402–408.
Lomovskaya, N.D., Mkrtumian, N.M., Gostimskaya, N.L., Danilenko, V.N., 1972. Characterization of temperate actinophage phiC31 isolated from *Streptomyces coelicolor* A3(2). J. Virol. 9, 258–262.
Luo, Y.Z., Li, B.Z., Liu, D., Zhang, L., Chen, Y., Jia, B., Zeng, B.X., Zhao, H.M., Yuan, Y.J., 2015. Engineered biosynthesis of natural products in heterologous hosts. Chem. Soc. Rev. 44, 5265–5290.
Merrick, C.A., Zhao, J., Rosser, S.J., 2018. Serine integrases: advancing synthetic biology. ACS Synth. Biol. 7, 299–310.
Morita, K., Yamamoto, T., Fusada, N., Komatsu, M., Ikeda, H., Hirano, N., Takahashi, H., 2009. The site-specific recombination system of actinophage TG1. FEMS Microbiol. Lett. 297, 234–240.
Murakami, T., Burian, J., Yanai, K., Bibb, M.J., Thompson, C.J., 2011. A system for the targeted amplification of bacterial gene clusters multiplies antibiotic yield in *Streptomyces coelicolor*. Proc. Natl. Acad. Sci. USA 108, 16020–16025.
Nepal, K.K., Wang, G., 2018. Streptomycetes: surrogate hosts for the genetic manipulation of biosynthetic gene clusters and production of natural products. Biotechnol. Adv. https://doi.org/10.1016/j.biotechadv.2018.10.003.
Nielsen, J., Keasling, J.D., 2016. Engineering cellular metabolism. Cell 164, 1185–1197.
Niu, G.Q., 2018. Genomics-driven natural product discovery in actinomycetes. Trends Biotechnol. 36, 238–241.
Nonaka, K., Kumasaka, C., Okamoto, Y., Maruyama, F., Yoshikawa, H., 1999. Bioconversion of milbemycin-related compounds: biosynthetic pathway of milbemycins. J. Antibiot. 52, 109–116.
Olano, C., Lombo, F., Mendez, C., Salas, J.A., 2008. Improving production of bioactive secondary metabolites in actinomycetes by metabolic engineering. Metab. Eng. 10, 281–292.
Ou, B.M., Garcia, C., Wang, Y.J., Zhang, W.P., Zhu, G.Q., 2018. Techniques for chromosomal integration and expression optimization in *Escherichia coli*. Biotechnol. Bioeng. https://doi.org/10.1002/bit.26790.
Roquet, N., Soleimany, A.P., Ferris, A.C., Aaronson, S., Lu, T.K., 2016. Synthetic recombinase-based state machines in living cells. Science 353, aad8559.
Ryu, Y.G., Butler, M.J., Chater, K.F., Lee, K.J., 2006. Engineering of primary carbohydrate metabolism for increased production of actinorhodin in *Streptomyces coelicolor*. Appl. Environ. Microbiol. 72, 7132–7139.
Shapiro, R.S., Chavez, A., Collins, J.J., 2018. CRISPR-based genomic tools for the manipulation of genetically intractable microorganisms. Nat. Rev. Microbiol. 16, 333–339.
Shi, S.B., Liang, Y.Y., Zhang, M.Z.M., Ang, E.L., Zhao, H.M., 2016. A highly efficient single-step, markerless strategy for multi-copy chromosomal integration of large biochemical pathways in *Saccharomyces cerevisiae*. Metab. Eng. 33, 19–27.
Siuti, P., Yazbek, J., Lu, T.K., 2013. Synthetic circuits integrating logic and memory in living cells. Nat. Biotechnol. 31, 448–452.
Smanski, M.J., Zhou, H., Claesen, J., Shen, B., Fischbach, M.A., Voigt, C.A., 2016.

Synthetic biology to access and expand nature's chemical diversity. Nat. Rev. Microbiol. 14, 135–149.
Smith, M.C., 2015. Phage-encoded serine integrases and other large serine recombinases. Microbiol. Spectr. 3, 1–19.
St-Pierre, F., Cui, L., Priest, D.G., Endy, D., Dodd, I.B., Shearwin, K.E., 2013. One-step cloning and chromosomal integration of DNA. ACS Synth. Biol. 2, 537–541.
Stark, W.M., 2017. Making serine integrases work for us. Curr. Opin. Microbiol. 38, 130–136.
Takiguchi, Y., Mishima, H., Okuda, M., Terao, M., 1980. Milbemycins, a new family of macrolide antibiotics-fermentation, isolation and physicochemical properties. J. Antibiot. 33, 1120–1127.
Tyo, K.E.J., Ajikumar, P.K., Stephanopoulos, G., 2009. Stabilized gene duplication enables long-term selection-free heterologous pathway expression. Nat. Biotechnol. 27, 760–U115.
Van Mellaert, L., Mei, L.J., Lammertyn, E., Schacht, S., Anne, J., 1998. Site-specific integration of bacteriophage VWB genome into *Streptomyces venezuelae* and construction of a VWB-based integrative vector. Microbiol-Sgm. 144, 3351–3358.
Wang, R., Mast, Y., Wang, J., Zhang, W.W., Zhao, G.P., Wohlleben, W., Lu, Y.H., Jiang, W.H., 2013a. Identification of two-component system AfsQ1/Q2 regulon and its cross-regulation with GlnR in *Streptomyces coelicolor*. Mol. Microbiol. 87, 30–48.
Wang, W.S., Li, X., Wang, J., Xiang, S.H., Feng, X.Z., Yang, K.Q., 2013b. An engineered strong promoter for *Streptomycetes*. Appl. Environ. Microbiol. 79, 4484–4492.
Wang, X.J., Yan, Y.J., Zhang, B., An, J., Wang, J.J., Tian, J., Jiang, L., Chen, Y.H., Huang, S.X., Yin, M., Zhang, J., Gao, A.L., Liu, C.X., Zhu, Z.X., Xiang, W.S., 2010. Genome sequence of the milbemycin-producing bacterium *Streptomyces bingchenggensis*. J. Bacteriol. 192, 4526–4527.
Weber, T., Charusanti, P., Musiol-Kroll, E.M., Jiang, X.L., Tong, Y.J., Kim, H.U., Lee, S.Y., 2015. Metabolic engineering of antibiotic factories: new tools for antibiotic production in actinomycetes. Trends Biotechnol. 33, 15–26.
Xu, M., Wang, Y.M., Zhao, Z.L., Gao, G.X., Huang, S.X., Kang, Q.J., He, X.Y., Lin, S.J., Pang, X.H., Deng, Z.X., Tao, M.F., 2016. Functional genome mining for metabolites encoded by large gene clusters through heterologous expression of a whole-genome bacterial artificial chromosome library in *Streptomyces* spp. Appl. Environ. Microbiol. 82, 5795–5805.
Yamanaka, K., Reynolds, K.A., Kersten, R.D., Ryan, K.S., Gonzalez, D.J., Nizet, V., Dorrestein, P.C., Moore, B.S., 2014. Direct cloning and refactoring of a silent lipopeptide biosynthetic gene cluster yields the antibiotic taromycin A. Proc. Natl. Acad. Sci. USA 111, 1957–1962.
Yang, L., Nielsen, A.A.K., Fernandez-Rodriguez, J., McClune, C.J., Laub, M.T., Lu, T.K., Voigtwill, C.A., 2014. Permanent genetic memory with > 1-byte capacity. Nat. Methods 11, 1261–1266.
Zhang, L., Zhao, G.P., Ding, X.M., 2011. Tandem assembly of the epothilone biosynthetic gene cluster by *in vitro* site-specific recombination. Sci. Rep. 1, 141.
Zhang, M.M., Wang, Y.J., Ang, E.L., Zhao, H.M., 2016. Engineering microbial hosts for production of bacterial natural products. Nat. Prod. Rep. 33, 963–987.